Flexible membrane structures for wave energy harvesting: A review of the developments, materials and computational modelling approaches

Ieuan Collins[a], Mokarram Hossain[a,*], Wulf Dettmer[a], Ian Masters[a]

[a] *Zienkiewicz Centre for Computational Engineering, Faculty of Science and Engineering, Swansea University, SA1 8EN, United Kingdom*

Abstract

In the last decade, there has been a growing trend towards flexible body wave energy converters (WECs) enabled by rubber-like elastomeric composite membrane structures that can simplify all aspects of WEC design. Currently, there are few literature studies detailing the implementations of membranes into WEC design. This paper aims to overcome this by reviewing the developments, material selection and modelling procedures for novel membrane based wave energy converters (mWECs), providing the reader with a comprehensive overview of the current state of the technology. In the first half of this paper, all of the possible WEC implementation areas are reviewed which include the primary mover, power take-off (PTO) and other sub-assembly systems. For the primary mover, the review has identified three main working surface approaches using membranes, these are: air-filled cells, water filled tubes and tethered carpets; which aim to reduce peak loads for enhanced reliability and survivability. In other areas, the PTO of WECs can benefit from using soft dielectric elastomer generators (DEGs) which offer a simpler designs compared with conventional mechanical turbomachinery. These have been implemented into the membrane working surface as well as replacing the PTO in existing WEC architectures. In the second half of the paper, a discussion is made on the material selection requirements with a few possible compositions presented. Following this, the potential modelling procedures for these devices is detailed. The device numerical models have altered existing procedures to take into account the non-linearities caused by the membrane interface and membrane PTO damping.

Keywords: Wave Energy Harvesting, Flexible Membrane, Elastomeric Membranes, Dielectric Elastomer Generators, Fluid-structure Interaction

Word Count. 11428

Abbreviations. Wave Energy Converter (WEC), Membrane Wave Energy Converter (mWEC), Dielectric Elastomer Generator (DEG), Power Take-Off (PTO), Technology Readiness Level (TRL), Levelised Cost of Energy (LCOE), Megawatts (MW), Pressure-Differential (PD), Oscillating Water Column (OWC), Fluid-Structure Interaction (FSI), Computaional Fluid Dynamics (CFD), Computational Solid Dynamics (CSD), Boundary Element Method (BEM), Finite Element Method (FEM), Arbitrary-Langrangian-Eulerian (ALE)

*Corresponding author

Email addresses: 793350@swansea.ac.uk (Ieuan Collins), mokarram.hossain@swansea.ac.uk (Mokarram Hossain), wulf.dettmer@swansea.ac.uk (Wulf Dettmer), i.masters@swansea.ac.uk (Ian Masters)

1. Introduction

Tackling climate change is a major challenge facing humans in the 21^{st} century. To achieve the goals set out by the United Nations and the Paris Climate Change Agreement, a significant portion of energy will have to come from renewable resources by 2050. Much of the development of renewable technologies can be dated to the aftermath of the 1973 oil crisis, where scientists, inventors and governments promoted the idea of harvesting energy from the sun, wind and ocean [1, 2]. In recent years, solar, and wind have been become attractive options due to their low environmental impact and reduced cost, and are starting to outperform fossil fuels [3]. On the other hand, wave energy has struggled to have the same success, even though the wave energy resource is significant [4] and could supply 10-20 % of the world's energy demand [5]. The cost of wave energy is significantly higher than that of wind and solar. One possible reason for the high levelized cost of energy (LCOE) is due to the lack of convergence in the wave sector. As a result, there is no market leader, and more designs are continually being developed [6–8]. Conventional WEC designs use a rigid-body system for the interface with the waves. These designs transfer the mechanical motion to a point-load power-take-off (PTO) system, typically a form of mechanical turbo-machinery which drives an electro-magnetic generator similar to wind and tidal based systems [9]. The development of a WEC follows five stages based on the technology readiness level (TRL), as identified by Heller et al. [10]. The initial 3 stages focus on developing laboratory tests and computational models to scaled sea trial testing (TRL 1-6). Stage 4 (TRL 7-8) focuses on a full-scale prototype sea trial testing and stage 5 (TRL 9) is an economic validation whereby several units are tested at sea for an extended period. At the time of writing, only two wave energy designs have made it to the commercial demonstration (stage 5, as identified), these being Pelamis [11] and Wello Penguin [12, 13]. It is speculated that part of reason for lack of progressed designs is due to the inherent challenge of using a rigid-body system with a complex component energy harvesting chain in a marine environment. The high loads and corrosive mechanisms are not well suited to metallic machinery, resulting in premature fatigue failures. Therefore, designs are large, heavy and often *'over-engineered'* to meet reliability standards, meaning they are typically costly and have poor adaptability to the wave climate.

Recent trends have re-evaluated WEC design by focusing on flexible bodies which aim to deliver a breakthrough in the marketplace by addressing the reliability and survivability issues facing conventional designs whilst providing greater conversion efficiency [9, 14]. Flexible body designs involve using a deformable structure comprising of an elastomeric composite, similar to other flexible marine structures like pressurised membranes for storage and transport of fluids [15], and breakwaters for coastal protection [16]. Starting from the mechanical interface with waves, a membrane working surface can accommodate external loading through changes in geometry, utilising an internal working fluid to transfer energy to the mechanical power take-off. However, the advent of dielectric elastomer generators (DEGs) means the PTO can be embedded into a stretchable material which allows the working surface and PTO to merge, resulting in a highly simplified design. Alternatively, DEGs have the ability to improve conventional architectures by replacing existing mechanical PTO systems. Flexible membrane Wave Energy Converter (mWEC) patents date back to the late 1970s [17]. Although recently, there is a renewed interest in this technology from tech-start ups and existing offshore companies [18–20]. Elastomer use in WECs is currently being investigated in the ELASTO project led by Edinburgh University and another project led by the National Renewable Energy Laboratory (NREL) [21, 22]. The majority of research into DEGs for WECs has been led

by the universities of Trento, Bologna, SSSUP (Pisa) and Edinburgh, working on the PolyWEC project and subsequent research funded by WETFEET and Wave Energy Scotland (WES) [23, 24].

There are in excess of 20 designs utilising a membrane as part of the device, and is seen as one of the biggest trends in the wave energy sector with more designs continuing to be developed. Previous wave energy reviews have considered rigid-body structures in great depth, see [6, 7, 25, 26]. An early materials study by Hudson [27] discusses the need to establish a better understanding of wear and fatigue properties of reinforced rubber membranes in the marine environment. Recent reports by the European Commission [28] and Wave Energy Scotland [29] discuss the challenges and opportunities of elastomeric membranes and DEGs in WEC design. More in-depth investigations on DEGs by Moretti et al [30] review DEG implementation into existing WEC architectures, with particular attention paid to the work undertaken in the PolyWEC project. Material science investigations into the optimum DEG materials for WECs remains a highly active field of research, with many works considering a range of soft rubber-like materials [31, 32].

The modelling procedures for WEC types range from simple reduced order frequency and time domain models, to highly complex multi-physics approaches and this also holds for membrane devices. This paper aims to bridge the gap of disciplines from the initial mWEC design to the appropriate material selection and finally introducing modelling methodologies applicable for a flexible body device. An overview of the different mWEC designs and developments is provided in Section 2. Section 3 details the material selection with attention paid to the mechanical, fatigue properties and environmental effects from the marine environment. In Section 4, the material models for flexible rubber materials are discussed with a review on the implementation into a fluid-structure methodology.

2. Design Implementations and Developments Review

Considering the energy harvesting chain, it is convenient to break a WEC into relevant component areas. These include the mechanical interface with the waves, the method of energy extraction and the combination of components to build a device, detailed below:

1. Primary Mover: The mechanical interface between the device and waves, which converts oncoming wave energy into useful mechanical motion.
2. Power Take-Off (PTO): The conversion of the mechanical motion into electrical energy which is transferred to the grid.
3. Non-harvesting sub-components: All of other components which make up the rest of the system such as mooring tethers, structural connections etc.

The possible harvesting chains for these component combinations are detailed in [33], where the choice of primary mover influences the possible PTO configuration. For detailed reviews on PTO systems, see [33, 34]. In Figure 1, the possible methods for the primary mover and PTO are identified along with other sub-assembly systems. One of the most versatile PTOs is conventional turbomachinery using a working fluid with long-standing usage in other energy harvesting devices. For WECs, both air or water turbines are possible and can be coupled to an accumulator, for example over-topping (WaveDragon) [35, 36] and Oscillating Water Column (Pico, Limpet) [37, 38]. Additionally, hydraulic PTOs using a working fluid such as oil or water have shown great potential and versatility since they can harvest energy between two moving bodies, resulting in numerous

configurations, for example attenuator (Pelamis) [39], terminator (Oyster) [40] and point absorber (WaveStar) [41]. On the other hand, mechanical transmission systems do not use a working fluid and instead rely on a moving body to drive a generator. This may be achieved through a piston pump (Ocean Grazer) [42, 43], moving mass (Wello Penguin) [13] or gear-up procedure [44, 45]. Direct-drive systems utilise a permanent magnet set-up allowing for contact-less energy mechanical energy transmission [46–48]. The remaining sub-assembly systems of a WEC are largely dependent on the footprint of the device. Fixed structures tend to be made out of concrete which house the prime mover and PTO, whereas floating bodies with many moving parts require additional shafts, mechanical connections, hulls and bearings to achieve energy extraction. The possibility of design simplification of all these mechanical systems can be achieved through elastomeric membrane structures at different stages of the energy harvesting chain, shown in blue on Figure 1. For instance the working surface (Section 2.1), the PTO (Section 2.2) and sub-assembly systems (Section 2.3). Suggestions are even being made for a zero machinery WEC whereby the working surface and PTO merge as one. Each area is categorised and reviewed in the following section.

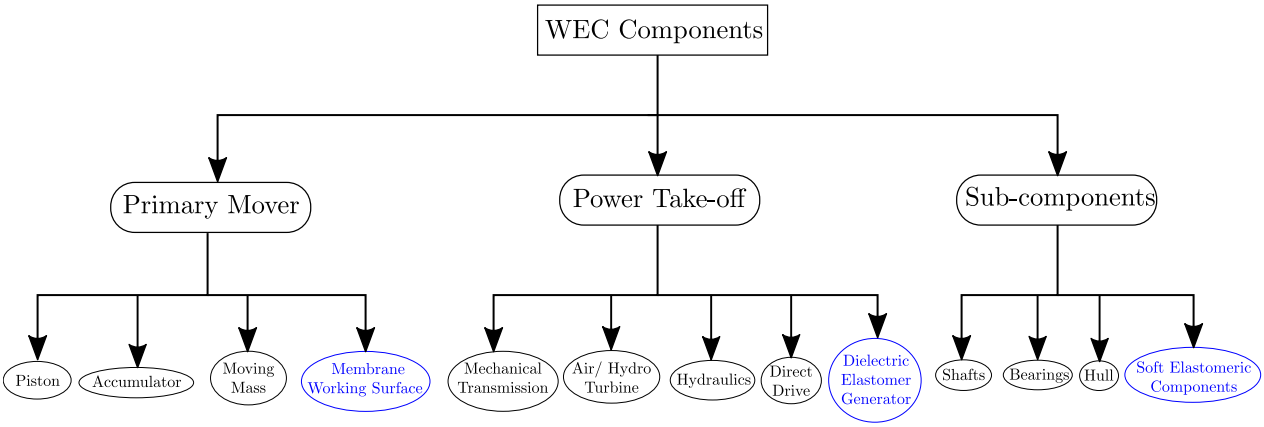

Figure 1. Mechanical components of a WEC.

2.1. Working Surface (Primary Mover)

Using a membrane as the working surface has resulted in radically different design configurations compared with conventional architectures. Herein, designs are classified based on how the working surface interacts with the waves and the internal working fluid. Based on this method, three main forms of working surface were identified: cellular (Section 2.1.1), tubular (Section 2.1.2) and carpet (Section 2.1.3) configurations, all located at different orientations relative to the oncoming waves. A full classification description and summary of developments in each area can be achieved by reference to Table 1.

2.1.1. Pneumatic Cell

A pneumatic cell device (Figure 2(a)) is a membrane with pinned boundary conditions covering an air-filled volume (cell). The external hydrodynamic pressure from the waves transfers energy to the membrane resulting in deformation forcing air out of the cell. The pressurised air is then captured by a PTO method, typically an air-turbine. The air is then recycled in a closed loop system which then re-inflates the membrane before the next oncoming wave.

Floating Attenuator. Early suggestions for a membrane working surface date back as far as the late 1970s with two floating configurations: the Lancaster Bag [17, 49] and Sea-Clam [50, 51]. The Lancaster Bag was suggested to be a 257 metre long concrete spine attenuator using rubber bags as the interface with the waves, motivated by the affordability and durability of rubber [52, 53]. However, the massive scale of the design meant it always remained at the concept stage, it has been speculated that progress halted due to the high structural costs, at 63 percent of the overall cost [54]. The Sea-Clam progressed further, starting as a terminator spine and later becoming a circular attenuator [55]. At 60 metres in diameter, the hull encompassed 12 rubber enclosed air filled cells, with a maximum power rating of 2.5 MW [50]. During the 1980s, various prototypes were tested on Loch Ness (UK), see Figure 5(c) [56, 57]. The recent introduction of an Oscillating Water Column (OWC) has replaced the membrane with Bucchi et al. [58] considering the structural integrity of this version [59]. A more recent development for attenuators is from AWS, which is similar in design to the Sea-Clam [60, 61]. During the 2010s, various prototype tests were performed on Loch Ness (UK) and at the MARIN hydrodynamic facility (Netherlands) [62]. Figure 5(f) shows a large-scale study of a single air-cell performed in Orkney (UK) [62, 63]. The proposed full-scale device has a length of 120 metres with a peak power output of 2.4 MW [18].

Submerged Pressure-Differential. The wave motion at the surface can be harvested through the pressure-differential (PD) at the sub-surface. A recent development in PD devices is the mWave by Bombora [64, 65]. The design uses a seabed-mounted concrete structure with 8 cells, 4 on either side of the spine, aligned diagonally to the oncoming wave crest. A large motivation for this configuration came from the idea of avoiding peak loads encountered at the surface for improved survivability. Novel experimental tests relying on geometric measurements through videogrammetry of a small-scale prototype have been performed by Orphin et al. [66] in shallow water at the Australian Maritime College Model Test Basin, which later were used for performance validation [67], see Figure 5(e). Modelling by Algie et al. [68] predicted the LCOE based on field data for a proposed location in Portugal. A 1.5 MW candidate device at 75 metres in length and a height of 4 metres is to be tested in Pembrokeshire (UK) [69]. The project aims to validate LCOE predictions made for the Portugal wave farm study [70] and demonstrate open ocean operation and survival during a winter deployment [71]. Another development from M3 Wave is the sea-floor PD mounted device called DMP. This device has two air-filled bags, separated by half a wave length which are located on the underside of a sea-floor mounted rigid structure [72, 73]. Scaled model testing has been performed off the Oregon coast (USA) [74, 75], shown in Figure 5(g). In [73], a power performance model was developed to support device design for a site off the coast of France.

Other. As part of an academic study, Plymouth University (UK) and partners considered various balloon configurations; two point absorbers [76, 77] and a submerged PD design [78]. In [79], they make a comparative study between these designs. Therein, it is shown that a deflatable balloon structure can increase the resonance period for point absorber designs. A small-scale prototype point absorber design was evaluated at the Plymouth Wave tank (UK) [76], see Figure 5(h). The PolyWEC project [23] considered DEG implementation into various existing architectures designs. One patent from the project was a submerged PD design; a membrane covering an insulated chamber in a submerged rigid-box structure [30, 80]. Instead of using a pneumatic PTO, the power is extracted through a DEG embedded in the moving membrane. The pressurisation of the chamber is controlled through a dynamic response variator, allowing the design to change its natural frequency to respond to a wide variety of sea states [80].

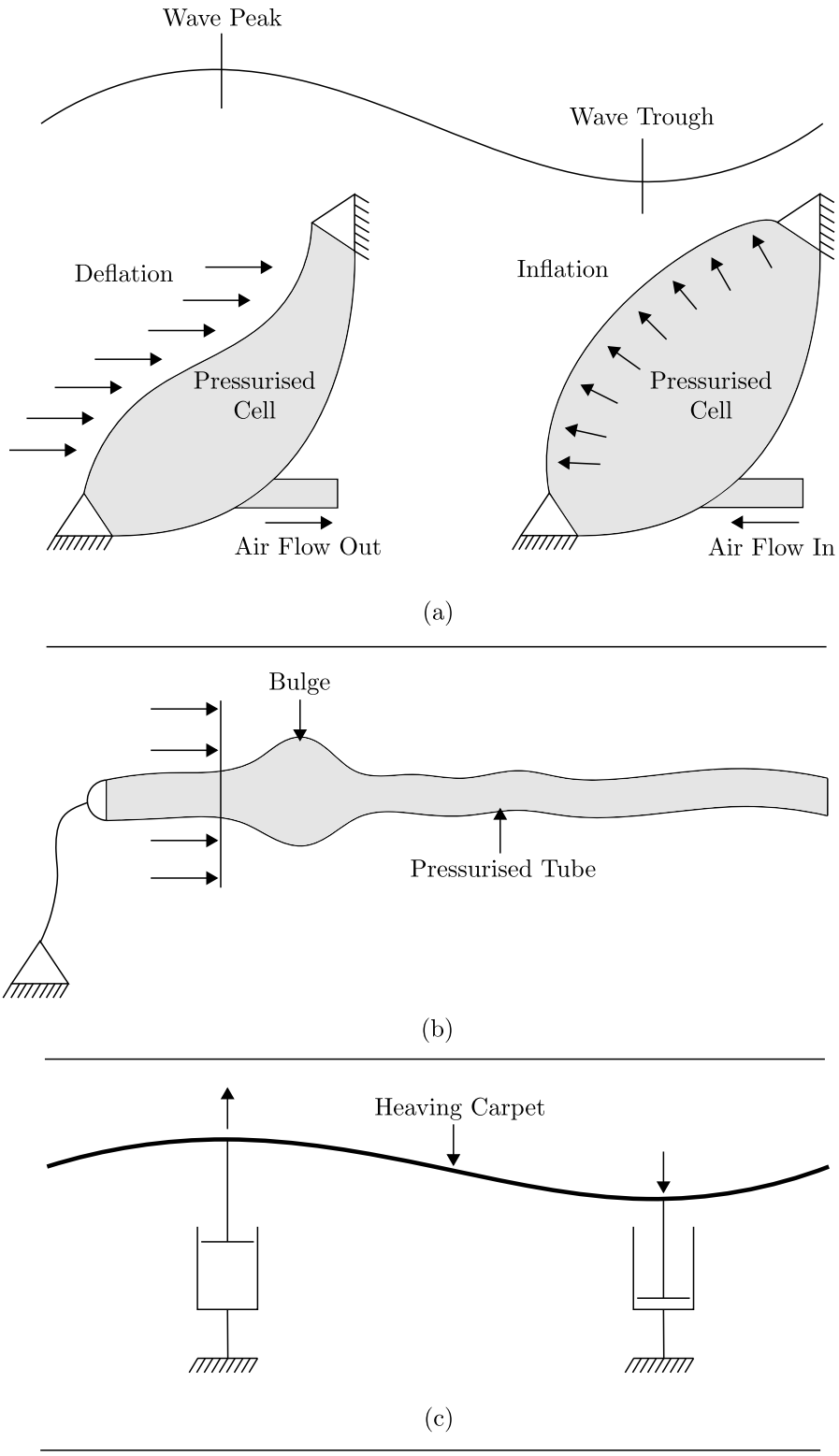

Figure 2. Membrane implementation into primary mover. (a) Pneumatic Cell, (b) Bulge Wave, (c) Tethered Carpet.

2.1.2. Bulge Wave

A bulge wave device (Figure 2(b)) is a tube filled with pressurised seawater which attenuates the waves near the surface. The tube is orientated perpendicular to the wave crest and moored to the seabed. As the wave crest passes alongside the tube, an internal bulge forms in front of the wave crest that grows progressively larger along the length of the tube, an idea conceived by Rainey and Farley [81]. The theory from Lighthill [82] states that a longitudinal pressure wave of the same velocity as the incident wave results in a transfer of energy to the tube which has later become known as the *'Bulge Wave'*. The internal working fluid bulge can be harvested at the stern of the tube. Alternatively, DEGs may be embedded into the tube material for continuous energy extraction.

Mechanical PTO. In 2006, Farley and Rainey invented the Anaconda device, developed further by Checkmate Seaenergy; the first patented bulge wave device [81, 83]. The initial design captured the bulge wave at the stern of the distensible tube through a hydro-turbine PTO [84]. Alongside the early development of the Anaconda design, another suggestion was made for a fully fabric tube, aptly named the Fabriconda [85]. Chaplin et al. [86] performed experimental tank tests on the Anaconda at Southampton University (UK), which showed good agreement between the measured power capture data and the one dimensional theory. Other scaled experimental prototypes were performed by Mendes et al. [87, 88] in Portugal for an air-turbine PTO method, estimating a power output of 0.5-1 MW per wave front. Recently, through funding from Wave Energy Scotland, the prototype versions of the device have been tested at FloWave, Edinburgh University (UK) and the Kelvin Lab, Strathclyde University (UK) [89], see Figure 5(a).

DEG PTO. The implementation of a DEG can remove all mechanical machinery in a bulge wave wave device. Two devices currently in development are from SBM [90, 91] and AWS [92, 93]. The SBM S3 contains DEG rings located along the length of the distensible tube, spaced between a traditional elastomeric material [91, 94], details on the operation of the DEG is provided in Section 2.2.1. A prototype scale device was tested in Monaco, which validated the energy harvesting cycle [91, 94], with more recent scaled tests performed at Ecole Centrale de Nantes (France) [95], see Figure 5(b). Using this experimental data as calibration, Babarit et al. [96] developed a numerical model which estimated a annual mean power of 100-200 kW for a 100 m tube. A full scale commercial design is suggested to be 6 MW for a 400 m tube [97]. The current plan is to test a 60 m long, 1.2 m in diameter prototype device off the coast of Monaco, submerged at approximately 4 metres [98]. The Electric Eel proposed by AWS, uses DEGs continuously embedded throughout the length of tube material [99]. The developers have suggested the integration of actuators and sensors into the membrane allows for the material stiffness to be altered depending on wave climate. A candidate device is scaled at 155 metres with a diameter of 7 metres, for a power production of 750 kW, while commercial designs are proposed to be 5.25 MW. The device remains at the early stage of development where patents have been granted [93, 99].

2.1.3. Tethered Carpet

A tethered carpet is a large surface membrane submerged with free end boundary conditions (Figure 2(c)), which is held in place via either tethers or hydraulic pistons. The carpet attenuates the wave motion by rising and falling with the wave peaks and troughs. It occupies a large surface area, and the free end boundary conditions allow for a high absorption efficiency. The heaving action of the carpet at various locations along its length can be captured with a hydraulic PTO.

The LilyPad [100, 101] and Wave Carpet [102, 103] are two devices proposed in the literature. The LilyPad is a floating dual-membrane attenuator, where the upper membrane is flexible while the lower membrane is much stiffer. The heaving action of the upper membrane is harvested with a hydraulic PTO positioned between the two membranes. The design is a patented concept with little known development in the literature. Another device called the Wave Carpet by CalWave is fully submerged and attached to the seabed. Initial analytical modelling by Alam [104] suggests the carpet has a broad operational bandwidth and is omnidirectional, absorbing wave energy above and below its surface. They theorise a possible theoretical efficiency of 100 %. Small-scale lab experiments by Lehmann et al. [103] confirm these findings showing a peak absorption efficiency of 99.3 %, see Figure 5(d). Although, the peak PTO efficiency was significantly lower at 42.3 %. The current plan is to deploy an open water version of this technology to understand the performance at commercial scale [105].

2.2. Membrane power take-off

Dielectric elastomers have the potential to replace traditional mechanical PTOs (Figure 1) in both novel and existing WEC architectures. In the past, other smart piezoelectric materials have been considered [106, 107], but were held back with bandwidth limitations. DEGs aim to overcome these limitations by operating over a much broader frequency range and have energy densities of 400 J/kg at laboratory scale; an order of magnitude greater than the piezoelectric ceramics and electromagnetic generators [108]. Studies speculate a mechanical efficiency conversion of up to 90 % [108, 109].

2.2.1. Operational principle

In a DEG, an elastomer is sandwiched between two compliant electrodes (terminals), taking the form of a capacitor, see Figure 3(b). When the material is stretched, there is corresponding reduction in the thickness causing the two electrodes to be closer and occupy a larger surface area, resulting in an increase in the capacitance. Energy is then harvested through this varying capacitance in one of two ways: by maintaining a constant voltage or applying constant charge [110, 111]. Herein we introduce the constant charge energy harvesting regime as used by two WECs in the literature [91, 112]. The harvesting cycle can be explained in 4 steps which correspond to Figure 3(a)[30, 94]:

- 1-2: The pressure from the waves causes stretching of the elastomer. This increases the effective area of the electrodes and decreases the distance between them, increasing capacitance.
- 2-3: Whilst at a maximum stretch, a constant charge is placed over the electrodes.
- 3-4: The pressure reduces after the wave has passed, allowing the elastomer to relax to its initial shape. Since the charge remains constant, the voltage increases.
- 4-1: The gained electrical energy is stored and the process is repeated for the next wave.

2.2.2. Implementation into WEC architectures

As discussed in Section 2.1, a DEG may be implemented into the membrane working surface for bulge wave and cellular configurations. Although existing architectures using rigid moving parts or a water accumulator structure may also benefit from this simplified PTO, detailed below.

Floating Buoys. The first application for a DEG in a WEC was in the form a stack inside a buoy developed by SRI International [113], with similar more recent concepts by Bosch [114, 115] and PolyWEC researchers [29, 116]. The heaving motion of the buoy causes compression and expansion of the DEG films, shown in Figure 4(a).

Oscillating Bodies. The surge converter [117] has seen alternative forms with DEG implementation suggested by SBM [118] and Moretti et al. [119, 120], replacing the hydraulic pump PTO. In [118], the energy from flap movement is harvested by a vertical stack of DEG films. Whereas, in [120] two parallelogram membranes are embedded either side of the moving flap which induces simple shear strain in the membrane.

Oscillating Water Column. The Oscillating Water Column (OWC) is one of the most developed conventional WEC architectures with full-scale working prototypes [37, 38]. Conventional OWCs use air-turbines, but DEGs may replace this system by covering the air-water column. The pressurisation from the moving water in the channel induces biaxial strain in the enclosed membrane, see Figure 4(b). The PolyWEC project and subsequent research have performed in-depth studies for OWCs of various configurations: fixed shoreline/ nearshore and floating. Moretti et al. [112] detail the investigations performed on a circular bottom-mounted OWC named Poly-A-OWC. Therein, a small-scale version of the design was tested at the FloWave facility, Edinburgh (UK), see Figure 5(i). The 2-3 W power output was estimated to be 300-440 kW at full-scale. Further research by Moretti et al. [121] has evaluated a fixed shoreline configuration at the Natural Ocean Engineering Laboratory (Reggio Calabria, Italy), to further evaluate their multi-physics model under real world conditions.

2.3. Sub-component systems

Soft and flexible membranes have numerous other uses throughout a WEC design. They may be used internally within a larger structure. For example, the Symphony device uses a roller membrane for substructure movement within a larger shell structure, replacing a complex mechanical bearing system [122]. Another example is the use of an inflatable membrane to change the footprint of a device. The Qoceant device uses an inflatable hull structure which may be inflated or deflated according to the wave climate [123].

Table 1: Summary of design implementations and developments in each area, where possible a power rating and patent reference is included for each design.

Application	Operational Type	Device	Orientation Classification	Depth Installation	Membrane Geometry	Power Take-Off (Rated Power)	Reference(s)
Membrane Working Surface	Pneumatic Cell	Lancaster Bag	Terminator	Sea Surface	Parallelogram	Air-Turbine (6.5 MW)	[17, 49, 52, 53]
		Sea-Clam	Attenuator	Sea Surface	Parallelogram	Air-Turbine (2.5 MW)	[50, 51, 55–57]
		AWS-III	Attenuator	Sea Surface	Parallelogram	Air-Turbine (2.4 MW)	[18, 60–62]
		Bombora mWave	Pressure-Differential	Fully Submerged	Parallelogram	Air-Turbine (1.5 MW)	[19, 64–66]
		M3 Wave DMP	Pressure-Differential	Fully Submerged	Parallelogram	Air-Turbine (150-500 kW)	[72–75]
		DrumWEC (PolyWEC Project)	Pressure-Differential	Fully Submerged	Circular	DEG	[23, 80]
		Air Bag (Plymouth Squid)	Point Absorber	Partially Submerged	Spherical	Air-Turbine	[76, 78]
	Bulge Wave	Anaconda	Attenuator	Near Surface	Cylindrical Tube	Hydro/Air-Turbine (0.5 - 1 MW)	[81, 83, 84, 86]
		Fabriconda	Attenuator	Near Surface	Cylindrical Tube	Hydro-Turbine	[85]
		SBM S3	Attenuator	Near Surface	Cylindrical Tube	DEG (1-6 MW)	[90, 91, 94, 97]
		AWS Electric Eel	Attenuator	Near Surface	Cylindrical Tube	DEG (0.75-5.25 MW)	[92, 93, 93, 99]
	Tethered Carpet	CalWave Wave Carpet	Pressure-Differential	Fully Submerged	Parallelogram	Hydraulic (90 - 148 kW/m)	[102–104]
		LilyPad	Attenuator	Partially Submerged	Parallelogram	Hydraulic	[100, 101]
Rigid Body WEC with Membrane PTO	Floating Buoy	SRI International Buoy	Point Absorber	Partially Submerged	Cylindrical Stacked	DEG	[113]
		Bosch/Wacker Buoy	Point Absorber	Partially Submerged	Cylindrical Stacked	DEG	[114, 115]
		PolyBuoy (PolyWEC Project)	Point Absorber	Partially Submerged	Cylindrical Stacked	DEG (267 kW)	[116]
	Oscillating Body	Nearshore WEC System (SBM Patent)	Terminator	Partially Submerged	Cylindrical Stacked	DEG	[117]
		PolySurge (PolyWEC Project)	Terminator	Partially Submerged	Parallelogram	DEG (0.7 - 1.5 MW)	[120]
	Oscillating Water Column	Poly-OWC	Point Absorber	Partially Submerged	Circular	DEG (140 - 560 kW)	[112, 121]
Rigid Body WECs with Membrane sub-components	Oscillating Body	Qoceant	Attenuator	Sea Surface	Parallelogram	-	[123]
		Symphony	Point Absorber	Fully Submerged	Cylindrical Tube	Hydro-Turbine	[122]

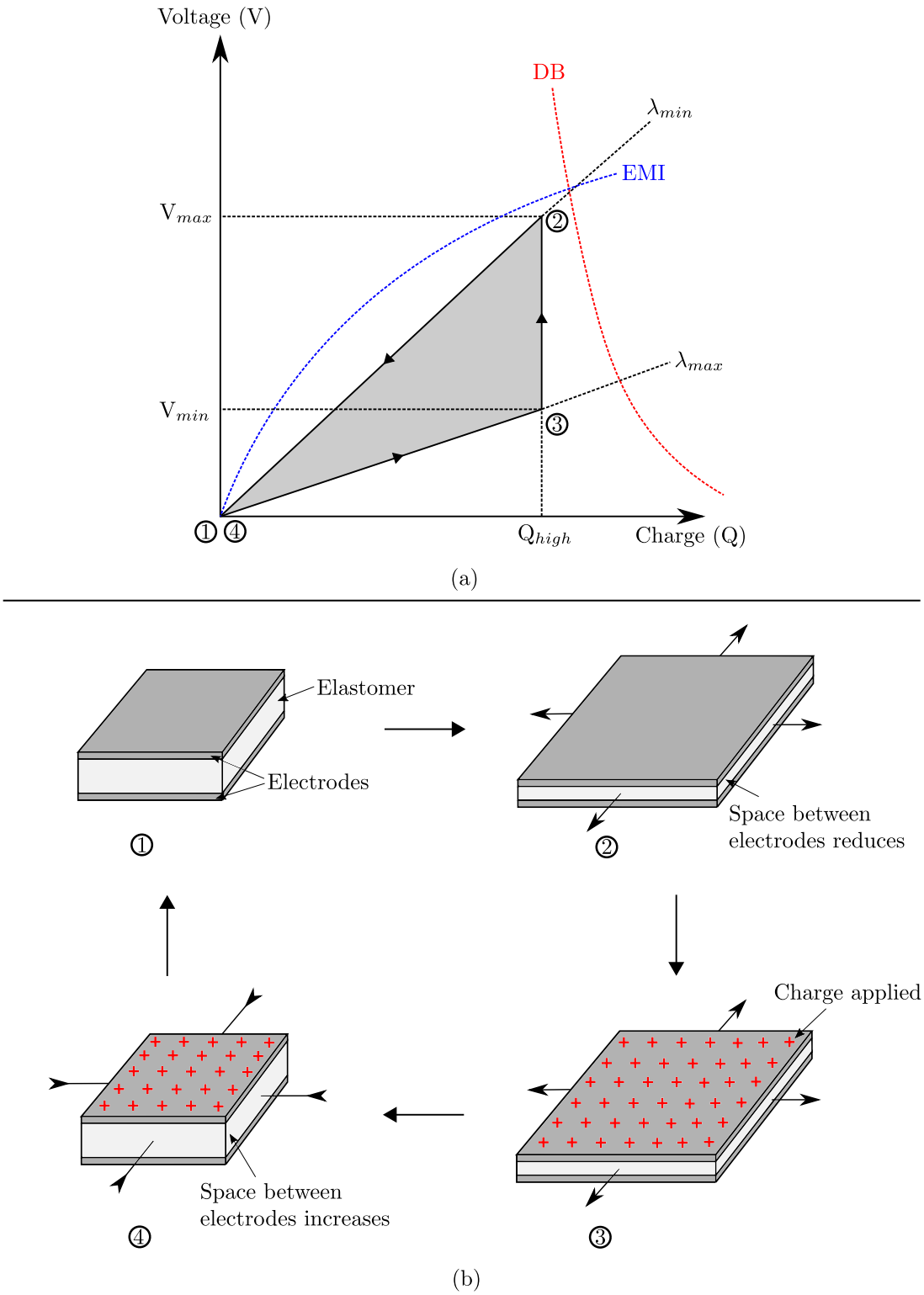

Figure 3. Constant charge dielectric elastomer harvesting process. (a) Constant charge energy harvesting process where EMI and DB refer to the electro-mechanical instability and dilectric breakdown, respectively. (b) Stretching of the dielectric elastomer corresponding to the constant charge harvesting regime.

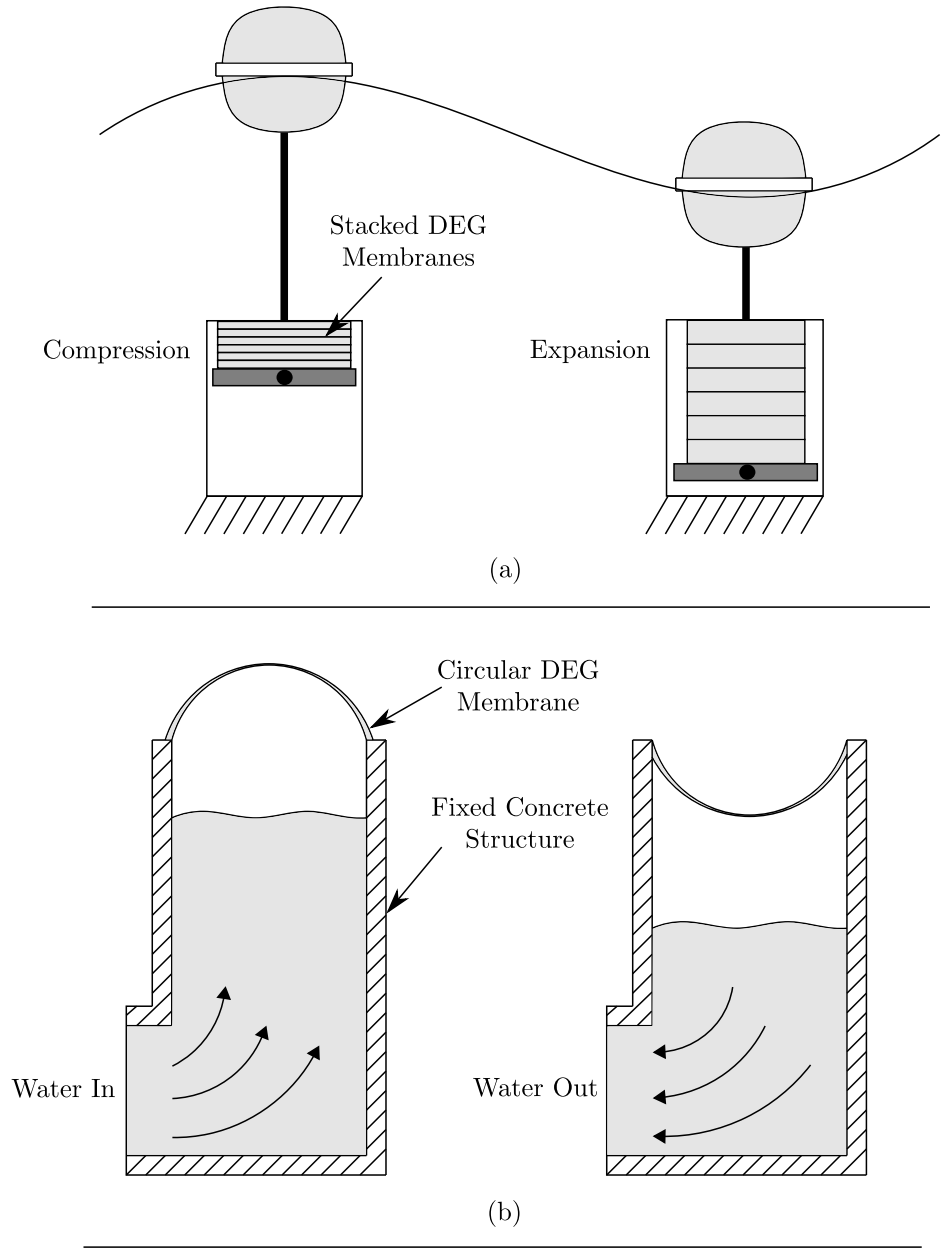

Figure 4. DEG implementation into existing WEC architectures. (a) Stacked membranes for point absorbing buoy, (b) circular membrane for an oscillating water column.

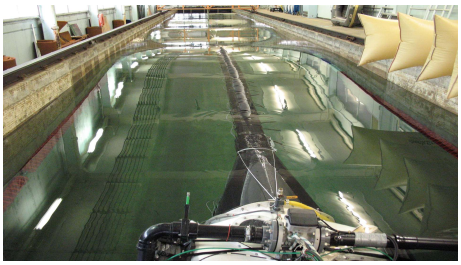

(a) Anaconda (Strathclyde Kelvin Hydrodynamics Laboratory, UK) [124]

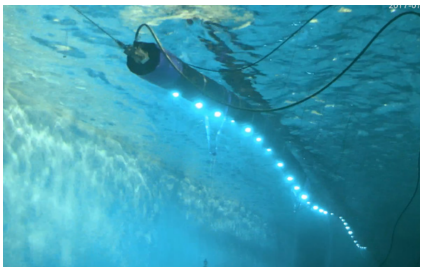

(b) SBM S3 (Ecole Centrale de Nantes, France) [95]

(c) Sea-Clam (Loch Ness, UK) [125]

(d) Wave Carpet (University of California, Berkeley TAFLab, USA) [103]

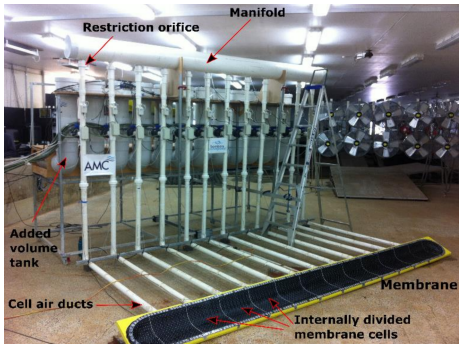

(e) Bombora mWave (Maritime College, Australia) [67]

(f) AWS-III Cassette Structure (Orkney, UK) [63]

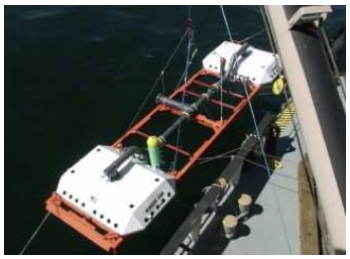

(g) M3 Wave DMP (Oregon, USA) [73]

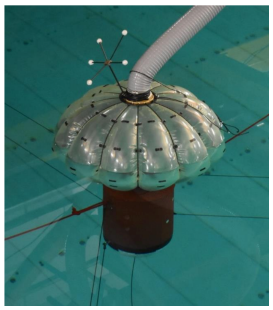

(h) Squid (Plymouth COAST Laboratory, UK) [79]

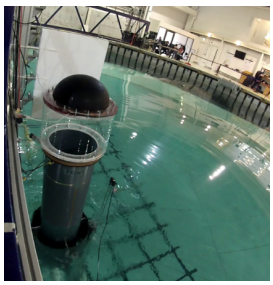

(i) Poly-A-OWC (Edinburgh FloWave Ocean Energy Research Facility, UK) [112]

Figure 5. List of prototype devices.

3. Material Selection

The design and formulation of an appropriate membrane is the subject of ongoing research by WEC developers. The ideal formulation is yet to be found with much of the work relying on experience in other sectors. This section reviews the important considerations regarding mechanical properties (Section 3.1), fatigue performance (Section 3.2) and unwanted instability phenomena (Section 3.3) in elastomeric materials. Then a few candidate formulations are presented for WEC membrane structures (Section 3.4).

3.1. Material Properties

The mechanical properties determine many operational factors of the device such as pressurisation and device dynamics. As identified by Moretti et al. [30] the four properties of merit are:

- Stretchability: Determines the maximum amount of strain before failure. For DEGs, a high stretchability is necessary to achieve a sufficient change in capacitance for energy harvesting. However, high stretch ranges is detrimental for the fatigue life (Section 3.2).
- Stiffness: Determines the amount a material deforms with respect to applied loading, which can influence pressurisation and device dynamics. Overly stiff materials will fail to attenuate the wave energy, while less than ideal stiff materials can suffer from instabilities (Section 3.3).
- Viscoelasticity: Determines the level of dissipation in the material in the form of hysteresis, stress relaxation and cyclic softening (Mullins effect) [126]. Viscous behaviour should be avoided to increase the energy conversion efficiency, minimise variations in response throughout operation and improve fatigue life.
- Electrical Properties: Determines the relative permittivity, dielectric breakdown strength and conductivity of the DEG. The relative permittivity is the amount of capacitance held at the plates, while the dielectric breakdown field is the level of voltage a material can withstand before becoming a conductor; both values need to be high for effective DEGs [127]. Conductivity of the material should be as low as possible to avoid '*leakage*' of electrical energy [128].

3.2. Fatigue and Durability

The fatigue and durability determines the tearing, abrasion and degradation resistance to the marine environment; all of which are important for membrane longevity and device reliability [129, 130]. The fatigue properties of elastomers in the marine environment are not well understood, although data from other sectors suggests good general performance. Factors which influence the fatigue life are the loads, environmental conditions and chemical formulation [131, 132]. Most fatigue studies of rubbers are based on uniaxial loading. However, biaxial is a more representative of expected loadings from the waves and internal working fluid, which may lead to a lower expected fatigue life if the control parameter is based on the maximum strain [133, 134]. An important aspect for ensuring optimum fatigue life is the strain crystallisation of rubber [131] as this results in strengthening of the polymer network after applied loading. This was shown in studies by [135, 136], where an improvement in the fatigue life was seen after applying a pre-strain whilst keeping the maximum amplitude load the same.

In addition to fatigue, the durability of elastomers in the marine environment are effected by the amount of water absorption and oxidation of the polymer [137, 138]. These ageing mechanisms can result in reductions in the stretchability, an increase in stiffness and reduction in the strength of the material [129, 139, 140]. There is little research on effect seawater and ageing has on fatigue life with only a few studies. The crack growth rate was found to be similar for natural rubber between air and seawater aged samples in [141, 142]. Recent in-depth studies have been performed by researchers under relaxing and non-relaxing conditions [143, 144]. In [143], they found a decrease in fatigue life for seawater when compared with air for non-relaxing conditions. While, a later study by [144] shows conflicting evidence for large strain amplitudes, with an improvement in fatigue life in seawater compared with air. They hypothesised this was due to the crystallisation of the rubber at higher strains, since the thermal properties of sea water are lower, the fatigue properties improve at high strains. A few studies have considered the electromechanical fatigue for DEGs, suggesting the imposed electrical field [91] and the operational environment [145] are the main influencing factors. So far, DEGs have shown the ability to perform in excess of several million cycles [91, 146–148]. In [148], 17.3 million cycles were achievable for a silicon elastomer with a 50% strain duty cycle, and in [91] silicone samples passed 15 million cycles for $0 - 80\%$ strain cycle. These studies suggest an excess of 4 years for 8 second waves, showing great promise in comparison to traditional PTOs. Future research needs to consider the biaxial variable amplitude loadings of membranes whilst considering the effect of seawater.

3.3. Material Instabilities

The instability of material refers to an unstable deformation with respect to loading, i.e., localised areas become highly deformed, while other areas remain unchanged. Two commonly observed examples in inflatable membranes are *Limit Points* and *Bifurcations* [149]:

- Limit Point: Consider the inflation of a circular membrane with pinned boundary conditions, as shown in Figure 6. The membrane is initially stiff for steps 1-2, requiring a high amount of pressure to increase in volume. As the inflation progresses, the pressure increments for radial stretching reduces. A maximum pressure is reached at step 3, referred to as the *critical pressure*. Beyond this volume, the pressure reduces while the volume still increases, referred to as a *limit point*.

- Bifurcations: Consider a water wave propagating through a cylindrical tube in figure Figure 7. For low pressures, the material exhibits uniform deformation (step 1). As the water bulge grows in size, the pressure acting on the membrane surface increases (step 2). At high levels of deformation, the load path changes resulting in strain accumulating in a localised area, referred to as an aneurysm (step 3). The aneurysm prevents the transfer of energy along the rest of the tube. Instead, the energy contributes to the aneurysm growth longitudinally, shown for the Anaconda wave energy device in [81].

The onset of instability is determined by the material stiffness, geometry and inflation fluid since these result in differences in the stretch distributions with applied loading [150–152]. Bifurcations can occur before or after the critical pressure, largely depending on the geometry of the membrane [153]. Increasing the pre-strain can induce instability sooner [154]. Therefore, higher pre-strains should be largely avoided to enable a higher pressurisation operational window. Limiting the extensibility of the material has been shown to result in stable inflations [155]. While increasing the stiffness, has allowed for higher operational pressures as demonstrated in a study on the Anaconda

WEC [156]. For a DEG membrane, the electrical properties can result in additional electromechanical instabilities [157–160]. To avoid this, DEGs must operate within a certain range before reaching electromechanical instability and dielectric breakdown field as shown in Figure 3(a).

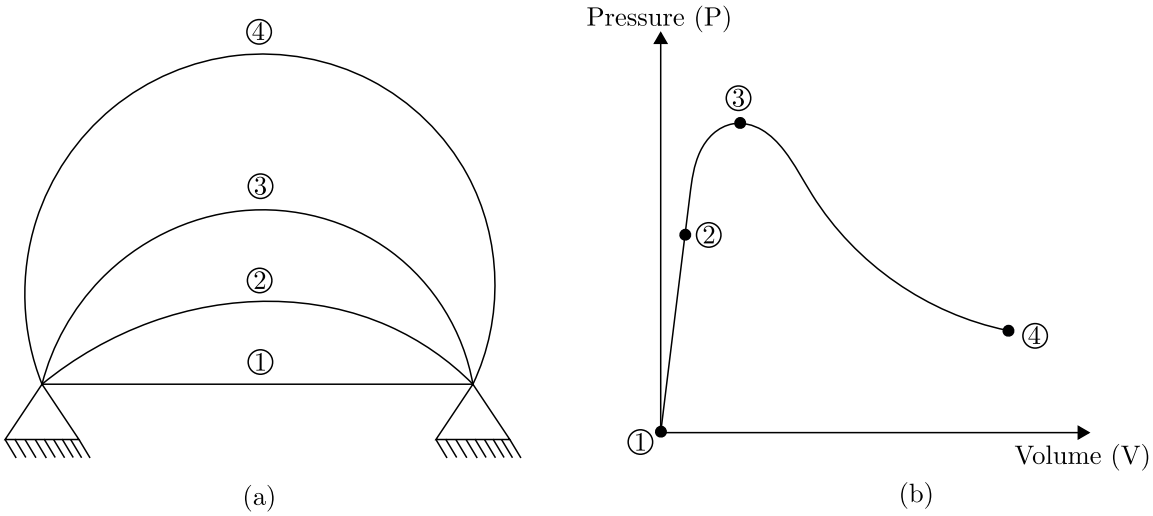

Figure 6. Limit Point Instability: Inflation of circular membrane.

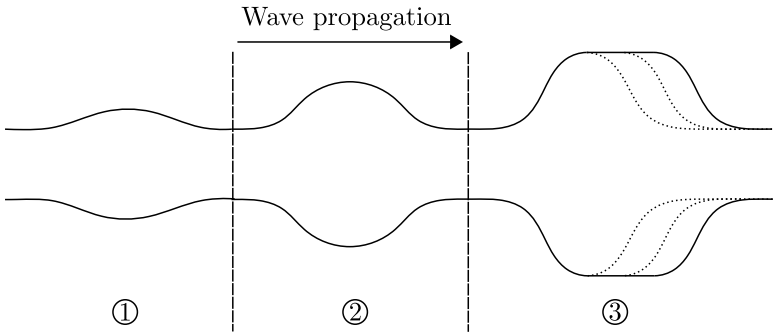

Figure 7. Bifurcation Instability: Inflation in a cylindrical tube.

3.4. Material Formulation

3.4.1. Base Material

The base material of an elastomeric membrane is made from a highly stretchable rubber-like polymer. The optimum material formulation is still the subject of research, requiring expertise from elastomer specialists. For sole primary mover implementation, natural rubbers seem to be the best option with excellent stretchability and low levels of hysteresis whilst at a low cost [32, 161, 162]. Silicones match natural rubber for mechanical properties, but the improved electrical properties and 3D printing manufacturing options mean they are better suited to DEG implementation [163–167]. For this reason, SBM have chosen silicone for their commercial S3 WEC design [91]. The downside is the significant extra cost when compared with natural rubber which is also viable for DEGs. Both silicones and natural rubbers have shown to have excellent fatigue properties [91, 168]. Other materials such as acrylics, in particular the VHB series by 3M, have been widely considered for DEG use as it offers the best stretchability and dielectric properties of readily available materials. It is often the choice of material for evaluating DEGs at laboratory scale [169]. However, due to high hysteresis, temperature sensitivity and high conductivity, these materials are not suitable for energy harvesting applications at a commercial level [128, 170]. Little research has been made into synthetic rubbers for WEC applications which have long-standing industry experience and good degradation resistance, but cannot match natural rubber tensile properties.

3.4.2. Material Reinforcement

The mechanical properties of rubber-like materials alone are usually not sufficient for most industrial applications. To obtain the desired stiffness to avoid the material instabilities and enhance fatigue life, rubbers are blended with other materials and fillers resulting in composites:

- Particle Filler: Small micro-particles are added throughout the elastomeric matrix to increase stiffness and tensile strength of the polymer, *e.g.*, carbon black and silica [171–173], see Figure 8(a). Furthermore, few recent studies successfully demonstrated that a synergy of various fillers such as graphene and carbon nanotubes, in addition to the traditional carbon black fillers, significantly enhanced the fatigue properties of filler-based elastomeric matrices, see [174, 175].
- Textile: Bonded to rubber to limit material extensibility, examples include rigid inflatable boat collars and tyres [29, 176], see Figure 8(b).
- Tendon: A polyamid tendon can be bonded to a polymer to increase stiffness in the direction of maximum strain, as suggested by the developers of the Sea-Clam and Anaconda [156, 177], see Figure 8(c).

3.4.3. DEG Considerations

DEG materials have the base material sandwiched between two conductive electrodes as shown in Figure 8(d). To harvest energy, the electrodes need to be stretchable yet remain conductive at large strains. Carbon powders and greases have been used at laboratory scale [178, 179], but are limited when scaling up to full-scale [30]. Potentially, carbon can be blended into an elastomeric matrix to create conductive rubber outer layers as suggested in [180]. Alternatively, researchers have investigated metallic electrodes. The electrodes can be corrugated to overcome the low elasticity and high stiffness of metals, see [181–183]. This corrugated approach was suggested in the SBM

bulge wave WEC [91, 94]. Alongside the base material, these electrodes must be able to endure tens of millions of cycles, with studies mentioned previously [146–148].

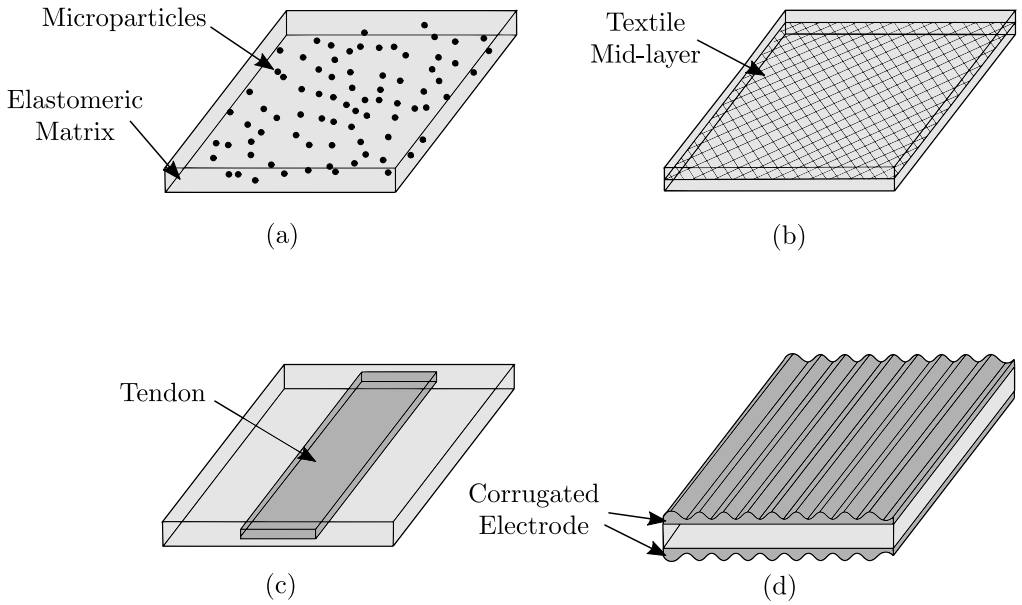

Figure 8. Membrane material compositions. (a) Microparticle reinforced elastomer, (b) textile lay-up reinforcement, (c) textile tendon in direction of maximum strain, (d) corrugated metallic electrodes

4. Device Modelling

Models of the interaction of the ocean with rigid body WECs have been under development for many years. These can be broadly separated into frequency domain models [184] and time domain models [185], alongside high fidelity computational dynamics approaches. For an excellent introduction to the topic, the reader is directed towards [186, 187]. Modelling a mWEC requires further considerations, in particular from a material modelling point of view, since the deformation regime of these designs is significantly large: in excess of 50% strain. Finite strain modelling approaches are needed to capture this behaviour through non-linear material models with various fitting parameters, section Section 4.1. Solving the fluid-structure interaction for mWECs poses additional challenges over existing designs, detailed in Section 4.2. The existing frequency domain and time domain approaches for rigid-body WECs, can be extended to include a deformable interface through simplifications as well as additional terms to describe the dynamical effects caused by membrane, working fluid and PTO. A review of the current methodologies is provided in Section 4.3. The high fidelity modelling procedures for the flexible fluid-structure interaction still pose a challenge numerically with limited usage at an industry level. A review on possible methods to overcome these challenges and the potential application to mWECs is presented in Section 4.4. A summary of all these approaches is then given in Table 2.

4.1. Material Modelling

For highly deformable rubber-like materials, the material modelling framework is based on large strain theory, in which the simplifications of infinitesimal theory (Hookean theory) are no longer

Table 2: Summary of modelling approaches, stating possible material models relevant to mWECs and viable fluid-structure interaction methodologies.

Modelling Method		Description	Accuracy and computational cost
Material	① Hyperelastic	A path dependent strain energy approach, which is broken down into volumetric and isochoric components. It builds on the linear-elastic theory by describing the non-linear stress-strain relationship using a polynomial function.	Low computational cost with material models built into existing commercial software. Accurate for simple early estimates for the stretchabilty of material, although energy losses from the material are ignored.
	② Viscoelastic	Decomposition of the deformation gradient into (hyper)elastic and viscous parts. Strain energy function is selected for each part. Requires extensive experimental calibration using stress relaxation and rate dependent loading tests.	Moderate computational cost which is dependent on the required number of Maxwell elements. Accurate for later material selections since it includes the dissipative behaviour of the material.
In combination:			
	③ - Electro	A decomposition of deformation gradient into mechanical and electrical parts for DEG WECs. The electrical component is based Maxwell's equations. Requires extensive experimental calibration using a DEG rig set-up measuring voltage/charge change with respect to loading. Used in combination with ① ②.	Moderate to high computational cost depending on the coupling method. Provides indication of power generation of DEGs with good accuracy although extensive experimental calibration is required.
	④ - Aging	A decomposition of strain energy function into unaged and fully aged parts. A time dependent decay function shifts the strain energy function from a virgin state to that of an aged one. Requires calibration with aged samples of different durations. Used in combination with ① ②.	Moderate to high computational cost depending on the coupling method and complexity of aging function. Provides indication of aging behaviour, although simple models are limited for including all possible degradation mechanisms.
	⑤ - Fatigue	Continuum damage and crack growth approaches are available. The prior uses a damage parameter to reduce stress which represents microvoid formation. While the latter is based on a J-integral representing a crack growth threshold energy. These models may be calibrated with crack growth experiments. Used in combination with ① ②.	High computational cost due to a large number of timesteps required. The accuracy is dependent on calibration with experimental data and loading conditions encountered, but the approach is useful for determining fatigue hotspots, crack growth characteristics and potential methods of mitigation.
Fluid-Structure Interaction: Reduced Order Approach	⑥ Steady-State	Static analysis for determining membrane shape under hydrostatic conditions. The hydrostatic force is applied to the membrane surface in a one or three dimensional analysis. The simplicity of this approach means it may be used with all of the above material modelling methods: ① ② ③ ④ ⑤.	Low computational cost in comparison to other approaches, since the dynamical effects of the fluid are ignored. The accuracy is inherently limited and is largely dependent on the calculated time dependent hydrostatic forces which may be obtained using any of the below methods.
	⑦ Frequency & Time Domain	Dynamic analysis can be used to determine modal shapes for mWEC devices using a BEM solver, usually based on linear wave theory. These approaches greatly verify depending on the device configuration and simplifications made. The most common approach is through generalised modes, where the natural frequencies of the device are calculated using an approach in ⑥, and is supplied to a hydrodynamical analyses for estimates on the device dynamics.	Moderate computational cost due to simplifications in the fluid-structure interaction by reducing the problem to a frequency or time domain model. The accuracy is adequate for early development stages and optimisation, but is limited due to the large interface displacements and unsteady flow effects surrounding the membrane.
Fluid-Structure Interaction: High Fidelity CFD-CSM Approach	⑧ Partitioned Solution Schemes	A continuum approach which solves the governing Navier-Stokes fluid equations coupled with a structural solver, often a CFD-FEM coupling. Partitioned solution schemes are widely available in commercial software, although are not well suited to mWEC applications. Partitioned iterative/ staggered coupling strategies show the most promise for mWECs with recent studies undertaken on flexible fluid-structure interaction problems. Used in combination with simple material models that converge easily: ① ②.	High computational cost due to added mass component which requires novel methods of coupling computation. The stability of these approaches is the main challenge for mWEC applications; overcoming this should provide for highly accurate simulations for estimates of the hydroelastic response.
	⑨ Monolithic Solution Schemes	Solves the continuum equations in one solver which overcomes many of added mass drawbacks of the above approach. It has shown to be a successful method for modelling many academic benchmark problems, although may be too computationally expensive for mWEC problems. Used in combination with simple material models that converge easily: ① ②.	Very high computational cost due to large system matrix requirements which may require a time consuming direct sparse solver. The stability and accuracy of this approach does show great promise for highly non-linear problems with significant added mass.

valid. The constitutive models for these materials are based on path independent *hyperelastic* strain energy functions, broken down into phenomenological and micro-mechanical approaches [188]. The prior uses polynomial functions to fit the material response of the experimental data. The latter uses physical characteristics. An introduction to hyperelastic models is provided in Section 4.1.1. Advanced finite strain models can include time-dependent dissipative behaviour as well as various other mechanisms, detailed in Section 4.1.2 and Section 4.1.3, respectively. These material models can then be implemented into a finite element framework for a structural analysis and coupled to an appropriate fluid-structure interaction method.

4.1.1. Hyperelastic models

Most polymers and their composites are deformable materials. Hence, they have to be modelled with the help of finite strain theory. The starting point for modelling a rubber-like material is the so-called strain energy function that relates to the deformation gradient, the key ingredient in finite strain theory. For isotropic hyperelastic materials, their properties are uniform in all directions. Therefore, the material response is invariant to the rotation of the reference configuration. Rubber-like materials are widely considered as incompressible materials (i.e., volume remains constant during deformation) in which the energy function can be expressed as volumetric and isochoric parts. The volumetric part of the energy function is introduced to impose the incompressibility assumption by using a parameter called hydrostatic pressure which is usually calculated using appropriate boundary conditions. Moreover, the strain energy function is either based on strain invariants or stretches of the Cauchy-Green strain tensor. Hence, the hyperelastic models for rubber-like materials can broadly be classified into two groups based on their formulations, i.e., invariant-based models and stretch-based models. The constitutive modelling of hyperelastic materials has been an active field of research for several decades since these models are also the building blocks of visco-hyperelastic models and for modelling soft biological tissues. Reviews of isotropic hyperelastic models are contained in Hossain et al. [188–190]. In order to demonstrate the key concepts of hyperelastic models and their calibrations, several experimental results were used, see [163] for details. Some polymers show a significant nonlinearity in their stress-strain relationship. Hence, a more complex strain energy function needs to be chosen. A three-parameter Carroll [191] strain energy function was widely selected thanks to its outstanding predictability in capturing hyperelastic experimental data for a wide range of polymeric materials, [188, 192].

4.1.2. Viscoelastic models

Rubber-like materials demonstrate strain rate and time-dependent viscoelastic behaviour. Hence, the hyperelastic model discussed above needs to be extended to capture time-dependent effects. The constitutive models for viscoelastic rubber-like polymers are broadly classified into two groups; phenomenological models and micromechanically-motivated models [193, 194]. One of the classical approaches in modelling viscoelasticity at finite strain from the phenomenological group is due to the so-called multiplicative decomposition of the deformation gradient, in which the gradient is decomposed into elastic and viscous parts. The decomposition of the deformation gradient resembles the spring-dashpot analogy in small-strain viscoelasticity, where the possibility of multiple viscous mechanisms in polymeric materials can be incorporated to the modelling framework, see Reese and Govindjee [195], Liao et al. [196]. The decomposition of the deformation gradient yields additional strain tensors. Motivated by the multiplicative decomposition of the deformation gradient, the strain energy function for a polymeric material is ideally decomposed into an elastic and a viscous parts. Sometimes, the observed experimental viscoelastic behaviour of polymers is

quite complex. In these cases, the number of Maxwell elements required is more than one. Using the second law of thermodynamics in the form of Clausius-Duhem inequality, an expression of the stress needs to be formulated. For tracking stress evolution with time in the case of viscoelastic materials, an evolution equation is required for the internal variable. Among others, a simple but widely used finite strain linear evolution equation is due to Linder et al. [193]. For more details about phenomenological evolution equations, see Lubliner [197], Reese and Govindjee [195], Amin et al. [198]. To obtain an update of the internal variable(s), an appropriate numerical solver is required. For parameters identification, data of a few different strain rates need to be selected. Once viscous parameters appearing in a model are identified, the model should be validated with another set of data which are not used in the parameters identification process, see [170, 199, 200].

4.1.3. Advanced Models

Advanced material models can consider a range of other effects, these include viscoelastic/viscoplastic damage, time-dependent environmental ageing and electro-mechanical coupling for DEGs. Continuum damage mechanics models simulate the non-linear damage accumulation on the basis of a reduction of effective stress caused by micro-voids, [201–203]. Ageing based models use a decay function to model the reaction and subsequent change in mechanical properties over time, see [199, 200, 204, 205]. Electro-mechanical models involve coupling mechanical deformation with the governing electrostatic equations, see [206]. The approach has been successfully used by WEC researchers for modelling the energy harvested by DEGs [112, 121, 169, 207, 208].

4.2. Fluid-Structure Interaction

The functionality of WEC devices rely on the deflection of membranes is fundamentally based on strongly coupled fluid-structure interaction (FSI), *i.e.*, any deformation of the structure triggers a response of the fluid flow and the vice versa. Hence, the simulation of the device requires the exchange of information between the fluid and the structural phases and neither subdomain can be solved independently of the other. This is fundamentally different from one-way coupling where information is passed only in one direction and the phases can be solved separately without the requirement for a coupling strategy.

A further complication arises from significant added-mass effects that are typically associated with mWECs. The term *'added mass'* denotes the amount of fluid mass that is entrained by the structure. Depending on the problem geometry and on the fluid/solid density ratio, the added mass effects can substantially increase or even dominate the inertia of the coupled system. Furthermore, added mass effects are stronger in problems involving incompressible fluids than in those featuring compressible fluids. Membrane WECs, similar to fluid-conveying elastic tubes, belong to the class of problems that feature an incompressible fluid (water) and a range of added mass modes. Figure 9, for instance, shows a number of modes of a pressurised membrane cell. Clearly, the low frequency modes require the acceleration of a much larger volume of fluid than the high frequency modes and therefore possess substantially more added mass. The mathematical derivation of similar modes in fluid-conveying tubes is presented, for instance, in [209].

As outlined in the preceding two paragraphs, the computer simulation strategy for an mWEC must be suitable for strongly coupled fluid-structure interaction problems which feature multiple added mass modes. Ideally, the numerical analyst would like to couple state-of-the-art strategies for computational fluid dynamics (CFD) and for computational solid dynamics (CSD). Section 4.4

describes why this still represents a challenge, despite today's advanced state and wide availability of engineering simulation software. More commonly, a reduced order modelling approach is chosen using simplified mathematical models that can be and have been formulated on the basis of various assumptions. The most common approaches are described in Section 4.3. For a comparison between reduced order and high fidelity approaches of floating structures, the reader is referred to [210].

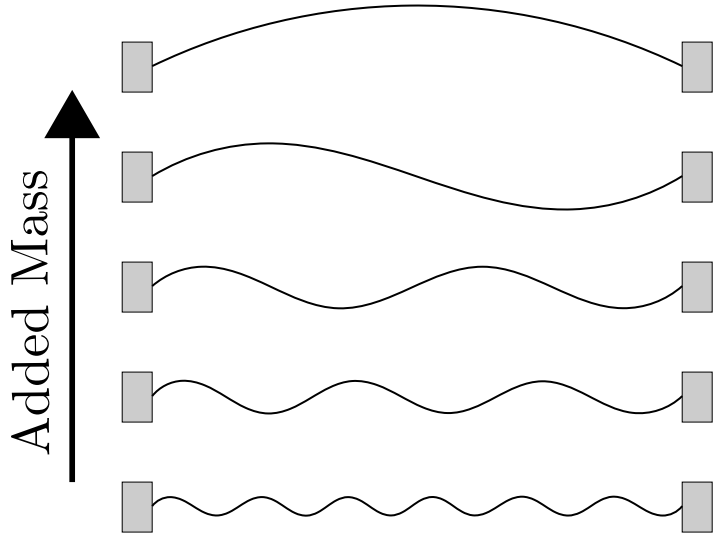

Figure 9. Selected eigenmodes with different amounts of added mass.

4.3. Reduced Order Models

4.3.1. Potential Flow Hydrodynamic Models

For early design estimates of the fluid-structure interaction of WECs, the starting point of analysis usually treats the fluid behaviour as linear using potential flow theory. For information on potential flow theory for WEC devices, the readers are referred to [46, 211, 212]. The numerical simulation may be based on a frequency or time domain procedure, where boundary element method (BEM) solvers are used, *e.g.*, WAMIT, Nemoh, WEC-Sim etc [185, 213, 214]. In most cases, a BEM solver is used to calculate the hydrodynamic forces acting on the body and to predict the dynamics of the device. The numerical simulation is much simpler for the frequency domain compared with the time domain, since it ignores non-linear affects arising from large amplitude motions and irregular sea states. Most rigid-body WECs have a maximum of 6 degrees of freedom per body, whereas a mWEC has significantly more and requires a greater effort for modelling the WEC dynamics. In addition, traditional solvers do not take into account geometric changes in membrane geometry and pumping of the internal working fluid. To overcome these issues researchers have developed bespoke methods for each device configuration which has usually involved extending the existing method to take into account these additional physical affects.

4.3.2. Steady State Models

If the system inertia is neglected, the response of a WEC device can be computed as a sequence of quasi-static configurations. The Bernoulli equation may be used to calculate a series of time dependent hydrostatic forces acting on the structure. This simplification removes the issue of the added mass phenomenon by neglecting the dynamic effects of the fluid. The literature is abundant

with quasi-static FSI analysis on membranes, see [215–219]. Such steady state analyses alone are only useful for sizing and for preliminary design. However, the results from a modal analysis of the structure may feed into a dynamical procedure in Section 4.3.3.

4.3.3. Frequency and Time Domain Models

Dynamic system models take into account the effects of inertia of the WEC. By reducing the three dimensional WEC system to suitable sets of excitation, state and response variables it is often possible to formulate a set of evolution equations that can be integrated numerically. The resulting models may be sufficiently accurate to allow for the preliminary design of the WEC. Such an approach was followed for instance in [220], where the physical affects of the Bombora WEC were broken down into forces for external hydrodynamics, internal air pressure and non-linear hydrostatic stiffness of membrane deflection. These forces were then equated to the external added mass of the water multiplied by the acceleration of the membrane. This complex frequency dependent procedure was simplified by assuming a series of idealised membrane shapes. A finite element membrane model was loaded by a hydrostatic external pressure field used to determine the hydrostatic stiffness of the membrane. The simplified membrane deformation shapes were then used for the calculation of the membrane hydrodynamic coefficients using Nemoh, where the power performance of the Bombora device is predicted for a potential site in Portugal. This performance model was validated with a 1:15 scale physical model through wave tank tests at the Australian Maritime College [67], showing good correlation for monochromatic wave tests.

For bulge wave devices, the hydroelastic response of the membrane is predicted using the tube distensibility equations. These are one dimensional models for pressure waves in fluid-conveying elastic tubes that were originally developed for simulations of the vascular system. These models are described, for instance, in [221]. This theory was applied to the Anaconda WEC [86], where the tube distensibility equation, originally proposed in [81], is formulated for a one dimensional dynamical model for bulge waves. Additional parameters such as the influence on surrounding water and PTO are considered as part of the analysis, with predictions for mean power. The model is compared to wave tank experiments on 1:25 scale device; quantitative agreement for the tube amplitudes was generally good and was improved further by altering the levels of hysteresis in the tube model. In [76, 222], a static and dynamical analysis is performed on a floating air bag WEC. The static analysis was used to calculate the equilibrium shape in still water with the axisymmetry of the device allowing for geometric simplifications. Following this, the frequency domain analysis was simplified by considering internal pressure changes in still water; compared with pumping experiments in still water in [223], showing reasonable agreement. The hydrodynamical forces were estimated using WAMIT based on this expected dynamical response.

A generalised modes approach is commonly used for deformable bodies [224], which has been successfully applied to various mWECs, see for instance [73, 225–227]. In [208] the authors build on the tube distensbility theory in [81, 86] and apply it to DEG SBM S3 bulge wave WEC, including additional physical effects relevant to this device configuration. The eigenmodes of vibration are calculated and following a modal decomposition procedure the hydroelastic response equations are derived. This numerical model compared with experiments for a 10 metre tube at the wave tank of Ecole Centrale de Nantes. The model showed good predictability, although the authors suggested various improvements such as including material non-linearities as well as additional fluid physical affects. Further work and improvements of this modelling approach are detailed in [228].

In [225, 226], they suggest a general modelling approach for mWECs, providing an easy point of access for the technology. The tool comprises of a quasi-static finite element analysis coupled with a dynamic analysis based in standard frequency domain utilising generalised modes. The tool uses the static analysis to determine the device membrane shape and stress under static loads, which feeds into a dynamic analysis. Additional terms depending on the device configuration are added to account for the mass, stiffness and damping associated with the membrane, internal working fluid effects, and PTO method. A case study bulge wave device analysis was performed and compared with the previous analysis of [208]. Similar wave response results were found to occur after the damping and mass components had been normalised using the maximum value for each mode shape. In [227], they suggest a method of including structural flexibility through a generalised modes approach in the time-domain modelling software: WEC-Sim. Similar to the above procedure, an eigenvalue analysis is used to identify the WEC natural frequencies and corresponding mode shapes. The corresponding mass, stiffness and damping matrices are constructed and supplied to WAMIT as generalised modes. WAMIT is used to calculate the hydrodynamic coefficients for the fluid-structure interaction which are then imported into WEC-Sim for a dynamic analysis of the device. This procedure is tested on two case studies and compared with a high fidelity computational fluid dynamics approach using STAR-CCM+, showing excellent agreement.

While these approaches are invaluable for early development stages, the accuracy of these approaches are limited. This is due to the inherent strong non-linearity and unsteady flow effects of a fluid-structure interaction system with large interface displacements. Additionally, high-fidelity approaches are better at capturing non-linear wave behaviour such as breaking wave effects. Therefore, it is advantageous to utilise high-fidelity modelling approaches for more informed design decisions.

4.4. High Fidelity Models

High fidelity fluid-structure interaction models require solving the governing equations for the fluid and solid at continuum level while resolving the strong coupling between the phases. In the following, an overview is provided over the numerical ingredients that constitute a viable numerical strategy.

4.4.1. Computational Fluid Dynamics

A variety of suitable finite element or finite volume based strategies is available for the modelling of the fluid flow that is governed by the incompressible Navier-Stokes equations and interacts with the WEC. Standard CFD strategies are formulated in an Eulerian setting in which the fluid domain remains fixed in space and the discretisation is based on a fixed spatial mesh or grid. However, a key feature of fluid-structure interaction is the deformation of the fluid domain. One of two approaches must be followed in order to adapt a CFD strategy to the moving domain.

The reference frame, mesh or grid, can be deformed continuously such that the interface boundary remains aligned with the structural boundary at all times. This requires the adjustment of the position of internal grid points. This continuous repositioning of the internal nodes is not governed by physics but by the desire to maintain a good mesh quality throughout the simulation. The most widely used methodologies are based on smoothing procedures or on a pseudo-elastic analogy where the mesh is assumed to behave like an elastic medium. The adjustments in the fluid-solver are minimal: The mesh velocity must be subtracted from the convective velocity and

the integration must be performed over the current cell or element configuration. Such methodologies are referred to as arbitrary-Lagrangian-Eulerian (ALE) formulations and are widely used, see for instance [229–233] and references therein. The advantages of ALE based strategies include fixed mesh connectivities throughout the simulation as well as accurate and robust resolution of boundary layers. The majority of commercial fluid-structure interaction software packages offer this technology. The drawbacks include excessive mesh distortion for large interface displacements and fixed problem topology. Hence, solid-solid contact and the opening or closing of orifices cannot naturally be integrated into the methodology.

The alternative approach is based on a spatially fixed fluid mesh or grid where the moving boundaries are tracked and the boundary conditions are imposed as constraints. Typically such strategies require the activation or deactivation of cells in every time step, depending on how they have been affected by the boundary movement. Such strategies naturally allow for topology changes and do not require the repositioning of mesh points. On the other hand, they require the imposition of boundary conditions inside the mesh and the stabilisation of cut cells. In recent years, these so-called immersed boundary methods have been advanced substantially within the research community and different versions have been developed, see, for instance, [234] and references therein. Recent applications to fluid-structure interaction are presented in, for instance, [235, 236].

4.4.2. Computational Solid Dynamics

In the vast majority of FSI simulations, the structural dynamics is modelled with well-established Lagrangian structural finite elements. Depending on the application, continuum, shell, membrane, beam or truss elements may be used. The finite element method for structural dynamics is well-established and widely available, see for instance [237, 238] and references therein.

4.4.3. Interface Conditions

At the fluid-solid interface, the fluid and solid boundary displacements must match at all times. Consequently the fluid velocities must equal the structural velocities. This is generally referred to as the *'kinematic consistency'* requirement. Furthermore, it is necessary that the traction forces exerted by the fluid flow on the structure are balanced by those exerted by the structure on the fluid flow. This is known as the *'equilibrium of the interface traction forces'*. In terms of finite element/volume meshes, suitable projection operators must be defined that allow the transfer of velocity, displacement and traction fields from one phase to the other. The solution strategy for the resulting algebraic system must resolve the strong coupling of the fluid flow and the structural dynamics. In the following, the two fundamental approaches, *i.e.* partitioned and monolithic solution strategies, are described.

4.4.4. Partitioned Solution Schemes

Partitioned solution schemes rely on the exchange of data across the interface boundary and on the separate execution of the fluid and the structural solvers. Partitioned solvers allow for the employment of existing sub-solver software and can be iterative or staggered. The latter class of solution algorithms is computationally most efficient, but also most challenging with regards to ensuring numerical stability. The coupling and the exchange of information across the interface can follow different approaches, some of which are described in the following. The overwhelming majority of available engineering software that offer the simulation of fluid-structure interaction employ the so-called iterative Dirichlet-Neumann coupling. Here, following a suitable initial guess, the structure

is loaded with the traction forces exerted by the fluid flow on the interface boundary. Subsequently, the interface displacements and velocities obtained from the structural dynamics solver are used as boundary conditions in the fluid solver. This procedure can be repeated until the desired accuracy requirements are met. However, since the inertia of the added mass is not accounted for in the computation of the interface displacements, the iteration does not converge in the presence of strong added mass effects. It is well-known and has been described in, for instance, [209, 239] and references therein that relaxation attenuates this shortcoming to a notable extent. However, as proven in [239], the Dirichlet-Neumann iterations are permissively inefficient and mostly diverge in the presence of the wide range of added mass modes that may be encountered in an mWEC. Hence, the authors are, at the time of writing, not aware of any successful high-fidelity simulations of a mWEC with the exception of the work [232] on the Bombora device. The latter is based on a modified Dirichlet-Neumann iteration implemented by the authors in OpenFOAM and ensures numerical stability by adding artificial damping to the membrane displacements. The authors also state that the number of iterations per time step is in excess of 100.

Alternative partitioned iterative or staggered coupling strategies employ different combinations of boundary conditions. Most notably this includes Robin or Nitsche type conditions, see for instance [240] and [241], respectively, and references therein. Some of these strategies are insensitive to added mass, but restricted to thin structures, where the structural mass reduces to point masses on the fluid boundary [242]. Their applicability to mWECs should be investigated. However, they have, to the knowledge of the authors, so far only been implemented and tested in research codes. The staggered Dirichlet-Neumann coupling with force predictor presented in [239, 243] is another candidate for the simulation of a mWEC. While it does not remove the added mass limit, it substantially increases the critical added mass effect without requiring intrusive software modification. A number of efficient staggered schemes based on compressible or artificially compressible fluid flow have been proposed in [244] and references therein. Finally, a number of relatively successful partitioned procedures have been developed from Quasi-Newton procedures, see for instance [245, 246] and references therein.

4.4.5. Monolithic Solution Schemes

Alternatively to partitioned coupling, the simulation may be based on monolithic solution procedures, where typically a Newton-Raphson procedure is used to solve simultaneously for all fluid and solid degrees of freedom, see for instance, [229, 230, 233, 247] and references therein. Such procedures are insensitive to the added mass phenomenon. However, they require the implementation of CFD and CSD solvers in a single software and the computation of non-standard cross derivatives. The conditioning of the large monolithic system matrix is typically worse than that of the sub-solvers matrices in a partitioned strategy. Hence, a direct sparse solver may be required. Altogether, for problems of industrial relevance, a monolithic solution strategy is typically far more computationally expensive than a partitioned strategy. Yet, the overwhelming advantage of monolithic solvers lies in their stability and robustness. The computational time required for the computation of the system matrix may be reduced by approximating or omitting selected cross derivatives. This may also lead to a sparser matrix pattern and benefit the linear equation solver. The effect of omitting certain derivatives on convergence is assessed, for instance, in [248].

5. Future Outlook

5.1. Design Opportunities and Development Challenges

The introduction of membrane structures for WECs has allowed for radically different designs, reducing the amount of mechanical machinery by using a novel flexible approach. The aim of these designs is to improve the reliability and maintainability of WEC design to ensure the LCOE is competitive with other renewables. The design opportunities over existing designs include:

- Structural: The structure can be deflated during periods of harsh loading to improve survivability against storms, as suggested by [19].
- Operational: Due to lower mechanical friction and larger surface capturing area, the operational bandwidth and absorption efficiency is improved, see [104].
- Design: A design may be simplified by using membranes in place of a rigid-body primary mover, mechanical machinery PTO, or a both as suggested by two developers [20, 93]. Simpler designs offer improved reliability and maintainability requirements, reducing overall operational costs.
- Deployment: Membranes are light in comparison to hard materials such as metals and concrete. They are also flexible and pressurised allowing for better storage solutions to the deployment site, such as reel configuration for bulge wave devices in [249].
- Footprint: For point absorber designs, the overall size of the device can reduce due to an increased resonance period [79]
- Manufacturing cost: The use of fewer components systems and materials has the potential to reduce the overall cost and supply-chain of WEC designs.

While the opportunities remain significant there are a number of challenges which remain to be overcome to progress designs further, these include:

- Prototype scaling: Experimental prototypes are used to validate early numerical models [250]. The membrane interface is difficult to scale under the conventional Froude scaling method due to the high non-linearity of scaling. Additionally, the soft interface may require geometric measurements, advanced video techniques have been used by [66, 76, 208].
- Novel Materials: Elastomeric materials for primary mover and PTO implementation require a better understanding. Notably, the membrane formulation needs to be optimised to ensure the desired mechanical and fatigue properties, as well as being manufactured on a large scale; discussed in detail in Section 5.2.
- Modelling Tools: Currently, there are a lack of modelling options due to the increased complexity of the membrane interface and membrane PTO damping, see section Section 5.3.
- Tidal Requirements: The size and location of the device will influence the adverse effects from the tides. Membranes with a large surface area are vulnerable to significant drag loads from tidal currents. This may put extra strain on the anchoring systems and therefore should be investigated. For free-floating bulge wave designs, there is the possibility the design will yaw in accordance with tidal currents which are not necessarily in the direction of the waves;

problematic from an energy harvesting perspective. Mooring solutions for tidal ranges are discussed in [251, 252]. In areas of high tidal range the changes in water depth are significant (over 5 metres). For nearshore seafloor mounted designs the pressure-differential and operational characteristics will change in accordance with low and high tides. To overcome this, a sea-level compensation system for WECs is suggested in [253].

At the time of writing, designs are progressing into TRL 5-7. These stages are critical for a better understanding of reliability, survivability and maintenance requirements in real-world conditions. From this, more accurate LCOE predictions can be made which will validate the competitiveness of these devices against other renewables.

5.2. Material Considerations

Elastomeric membranes require further research to bring them to higher levels of TRL for WEC applications. To progress industry knowledge further, several areas need to be addressed:

- Mechanical Properties: Natural and silicones rubbers have been identified as the best materials for WEC applications [32, 91]. The optimum amount of particle filler and composite reinforcement requires further research to ensure designs can operate in a wide pressurisation operational window, whilst avoiding material instabilities. The best solution currently available is to utilise the knowledge from other sectors using similar elastomeric structures, e.g. rubber dams, hovercraft skirts and automotive tyres.

- Fatigue and Durability: Natural and silicone rubber are known to have good fatigue properties in other sectors [148, 168]. At the present time, the effect of multi-axial fatigue coupled with the marine environment has little research, with limited facilities available to perform these tests. Ideally, material formulations should be evaluated with small-scale fatigue experiments, before going to larger scale accelerated life tests. This is an area requiring more facilities for making informed material selection.

- DEG Considerations: The development of a suitable electrode is the subject of ongoing research, two of the most viable options are conductive carbon layers and corrugated metallic electrodes [180, 181]. To achieve the desired electromechanical fatigue life, a compromise has to be made between the amount of harvested energy and lifetime of electrode since higher stretches and electrical fields result a in lower electrode life.

- Manufacturing Considerations: The scale of these membranes are potentially massive, in excess of 100 metres. Research into a suitable vulcanisation and material joining method is required to to ensure the material properties remain consistent throughout the membrane. Non-homogeneous mechanical properties may result in potential bifurcations and crack growth spots. It has been suggested full-scale DEG membranes are multi-layered (elastomer-electrode) where traditional vulcanising techniques are not applicable [30, 112]. Alternatively, novel 3D printing techniques may be required [166, 167].

5.3. Modelling Considerations

The modelling framework for conventional WEC designs has been established with the use of hydrodynamical software for early design estimates and CFD approaches for high-fidelity approaches. A membrane interface presents a significant challenge in terms of computational resources. To accurately model a mWEC, considerable research is needed in the following areas:

- Material Modelling: The material modelling framework for elastomers is well-established with many hyperelastic models [188–190] and complex time-dependent models available [195–197, 199]. The incorporation of multi-physics aspects such as seawater degradation, fatigue damage and electromechanical coupling can be achieved through various decomposition procedures, see [121, 203, 205, 206]. The challenge is the implementation of these models into finite element solvers, since they require many experimental parameters and verifications. Additionally, the high non-linearity means these models can suffer from convergence issues when performing an FSI analysis. Biaxial characterisation provides better data for model calibration of mWECs but the machinery to performance these tests is scarce. The material modelling process should increase in complexity with regards to selection of a suitable membrane material. At early stages where only the stretchability of the material is considered, it is recommended developers use hyperelastic models based on two to three parameters. Once a desired stretchability range is identified, later stages should consider the dissipative behaviour through the use of viscoelastic models. The fatigue life and degradation of the membrane throughout the operation can be considered at the final stages but will require simplifications in other parts of the FSI analysis using reduced order approaches.

- Reduced Order Modelling: Currently, there are no hydrodynamic software options available which natively consider flexible membranes as part of the analysis. Therefore, developers have chosen to develop bespoke models for device development, see [76, 86, 208, 220]. The problem with this approach is the resources, expertise and time required to develop individual bespoke models. The variation between methods also means the FSI results are not as easily comparable between devices. The most common and promising approach is through a generalised modes procedure. An eigenvalue analysis is performed to identify the natural frequencies of the mWEC, these deformation modes are supplied as custom degrees of freedom in a frequency domain BEM analysis. A generic software tool using this generalised modes procedure is being developed by [225, 226]. The tool aims to provide industry standardisation for FSI simulations for WECs involving a membrane interface whilst also allowing for easy entry for prospective developers.

- High-fidelity Modelling: The CFD-CSD simulations provide informed results for structural loading since all the unsteady flow effects are considered, however at the current time there remain significant challenges in terms of interface solving schemes. To authors knowledge, only one high-fidelity mWEC study has taken place [232]. Partitioned solution strategies that are insensitive to the added mass phenomenon show the most promise for WEC applications [239–241]. These methods are currently at early research development stages and not commercially available. Future research needs to develop tools for open source software, *e.g.* OpenFOAM, allowing for high fidelity simulations of mWEC designs for more informed loading and hydroelastic response estimates.

- Reliability Modelling: To evaluate the LCOE of the device, it is necessary to perform the reliability analysis of the interface structure based on loading from stochastic wave data. Conventional WEC design has well-established approaches which rely on calculating wave loads on structures through the above procedures, and using a damage accumulation rule for fatigue, see [254–258]. However, due to the limited options and highly non-linear damage accumulation, mWEC designs may require a more *'pragmatic'* approach to such an analysis. At this current time, it is recommended developers use frequency domain modelling utilising

generalised modes for the calculation of loading on the structure and the expected hydroelastic responses for a varied wave climate. Based on these loading estimates, the damage accumulation can be simulated through a non-linear finite strain damage model in a quasi-static modelling environment. A toolbox should be developed which allows for easy coupling between these analyses.

6. Conclusions

- This review has identified in excess of 20 instances of soft membrane structure use in WEC design. These have been implemented into the primary mover, PTO and other sub-component systems. The technological developments are summarised in Table 1. The capacity of most candidate designs is in 1-2.5 MW range, larger scale designs are expected to be up to 6 MW, with surface floating designs having the greatest power output potential. There are two designs nearing TRL 6 with sea-trials planned in the near-future.

- Natural rubber and silicone are the most appropriate materials for the primary mover and PTO, respectively. As both materials offer low levels of hysteresis and high stretchability, while the latter has superior electrical properties for DEG applications. These rubber materials are often combined with rigid materials to form a composite/fabric requiring further research investigations, though it is expected a mix of fillers, textiles and tendons will be utilised based on other sectors. An overview of potential composite options is given in Figure 8. Compliant electrodes for DEGs are the subject of research; conductive carbon and metallic electrodes appear promising. The appropriate manufacturing methods also have to be identified. It is expected 3D printing of silicones offers the best solution currently.

- The modelling of the rubber membrane material is possible through numerous well-established material models. However, there are few options available for coupling to an FSI solver since mWECs have additional challenges over existing designs. To overcome these challenges, various works have modified the existing frequency and time domain procedures to account for the membrane dynamics and internal working fluid. A generalised modes procedure is the most promising approach for future development tools. Little work has considered high-fidelity CFD approaches due to the limitations in computational hardware. Although, it has been identified the most viable high-fidelity approaches are novel partitioned solution schemes that are insensitive to the added mass phenomenon. Combining these approaches allows for reliability estimates of the structure where tools are still required to be developed. A summary of all the modelling relevant to mWECs is given in Table 2.

- Addressing these material and modelling challenges is key for progression of the TRL. Once this is achieved, more development opportunities and funding should be available for this second generation of WECs.

Acknowledgements

This research is supported by the Knowledge Economy Skills Scholarships (KESS 2). Knowledge Economy Skills Scholarships (KESS 2) is a pan-Wales higher level skills initiative led by Bangor University on behalf of the HE sector in Wales. It is part funded by the Welsh Government's

European Social Fund (ESF) convergence programme for West Wales and the Valleys. This study is also supported by EPSRC through the Supergen ORE Hub (EP/S000747/1), who have awarded funding for the Flexible Fund project Submerged bi-axial fatigue analysis for flexible membrane Wave Energy Converters (FF2021-1036).

References

[1] Lindquist H. The journey of reinventing the european electricity landscape. In: Renewable Energy Integration. Elsevier; 2017, p. 3–13.

[2] Salter SH, et al. Wave power. Nature 1974;249(5459):720–4.

[3] IRENA . Renewable power generation costs in 2018. International Renewable Energy Agency; Abu Dubai, UAE; 2019.

[4] IRENA . Wave energy technology brief. International Renewable Energy Agency; Abu Dubai, UAE; 2014.

[5] Aderinto T, Li H. Ocean wave energy converters: Status and challenges. Energies 2018;11(5):1250.

[6] Drew B, Plummer AR, Sahinkaya MN. A review of wave energy converter technology. Proceedings of the Institution of Mechanical Engineers, Part A: Journal of Power and Energy 2009;223(8):887–902.

[7] Clément A, McCullen P, Falcão A, Fiorentino A, Gardner F, Hammarlund K, et al. Wave energy in europe: current status and perspectives. Renewable and sustainable energy reviews 2002;6(5):405–31.

[8] The European Marine Energy Centre Ltd, Wave Devices. http://www.emec.org.uk/marine-energy/wave-devices; 2020 [Accessed 28 October 2020].

[9] Babarit A. Ocean wave energy conversion. Elsevier; 2018.

[10] Heller V. Development of wave devices from initial conception to commercial demonstration. In: Comprehensive Renewable Energy. Elsevier; 2012, p. 79–110.

[11] Yemm R, Pizer D, Retzler C, Henderson R. Pelamis: experience from concept to connection. Philosophical Transactions of the Royal Society A: Mathematical, Physical and Engineering Sciences 2012;370(1959):365–80.

[12] Wello, Clean energy from ocean waves. https://wello.eu/; 2020 [Accessed 28 October 2020].

[13] The European Marine Energy Centre Ltd, Wello Oy. http://www.emec.org.uk/about-us/wave-clients/wello-oy; 2020 [Accessed 28 October 2020].

[14] Pecher A, Kofoed J. Handbook of ocean wave energy. Springer Nature; 2017.

[15] Hawthorne WR. The early development of the dracone flexible barge. Proceedings of the institution of mechanical engineers 1961;175(1):52–83.

[16] Williams A, Geiger P, McDougal W. Flexible floating breakwater. Journal of waterway, port, coastal, and ocean engineering 1991;117(5):429–50.

[17] French M. Water wave energy conversion device using flexible membranes. U.S. Patent 4164383, Aug 14, 1979.

[18] AWS, AWS-III multi-cell wave power generator. https://www.awsocean.com/multi-cell-wave-power/; 2020 [Accessed 28 October 2020].

[19] Bombora, mWave. https://www.bomborawave.com/mwave; 2020 [Accessed 28 October 2020].

[20] SBM Offshore, Renewable energy. https://www.sbmoffshore.com/what-we-do/our-products/renewables/; 2020 [Accessed 28 October 2020].

[21] A feasibility study on Elastomeric based WECs (ELASTO). Tech. Rep.; University of Edinburgh and Wave Energy Scotland; 2018.

[22] NREL, Water Research, Flexible Materials with Distributed Energy Converters. https://www.nrel.gov/water/flexible-materials-distributed-energy-converters.html; 2020 [Accessed 29 May 2021].

[23] European Commision CORDIS EU research results, New mechanisms and concepts for exploiting electroactive Polymers for Wave Energy Conversion. https://cordis.europa.eu/project/id/309139/reporting; 2020 [Accessed 28 October 2018].

[24] WETFEET, WETFEET Project. http://www.wetfeet.eu/wetfeet-project/; 2020 [Accessed 28 October 2018].

[25] Falnes J. A review of wave-energy extraction. Marine structures 2007;20(4):185–201.

[26] Falcáo A. Wave energy utilization: A review of the technologies. Renewable and sustainable energy reviews 2010;14(3):899–918.

[27] Hudson J, Phillips D, Wilkins N. Materials aspects of wave energy converters. Journal of materials science 1980;15(6):1337–63.

[28] Workshop on identification of future emerging technologies in the ocean energy sector. Tech. Rep.; European Commission; 2018.

[29] Materials landscaping study. Tech. Rep.; Wave Energy Scotland; 2016.

[30] Moretti G, Herran M, Forehand D, Alves M, Jeffrey H, Vertechy R, et al. Advances in the development of dielectric elastomer generators for wave energy conversion. Renewable and Sustainable Energy Reviews 2020;117:109430.

[31] Maas J, Graf C. Dielectric elastomers for hydro power harvesting. Smart Materials and Structures 2012;21(6):064006.

[32] Kaltseis R, Keplinger C, Koh SJA, Baumgartner R, Goh YF, Ng WH, et al. Natural rubber for sustainable high-power electrical energy generation. RSC Advances 2014;4(53):27905–13.

[33] Têtu A. Power take-off systems for WECs. In: Handbook of ocean wave energy. Springer, Cham; 2017, p. 203–20.

[34] Liu Z, Zhang R, Xiao H, Wang X. Survey of the mechanisms of power take-off (PTO) devices of wave energy converters. Acta Mechanica Sinica 2020;36:644–58.

[35] Kofoed JP, Frigaard P, Friis-Madsen E, Sørensen HC. Prototype testing of the wave energy converter wave dragon. Renewable energy 2006;31(2):181–9.

[36] Margheritini L, Vicinanza D, Frigaard P. SSG wave energy converter: Design, reliability and hydraulic performance of an innovative overtopping device. Renewable Energy 2009;34(5):1371–80.

[37] Pecher A, Kofoed J, Le Crom I, Neumann F, Azevedo E, et al. Performance assessment of the Pico OWC power plant following the EquiMar Methodology. In: The Twenty-first International Offshore and Polar Engineering Conference. International Society of Offshore and Polar Engineers; 2011,.

[38] Heath T, Whittaker TJT, Boake CB. The design, construction and operation of the limpet wave energy converter (islay, scotland)[land installed marine powered energy transformer]. Proceedings of the 2001 Denmark) 2001;:49–55.

[39] Henderson R. Design, simulation, and testing of a novel hydraulic power take-off system for the pelamis wave energy converter. Renewable energy 2006;31(2):271–83.

[40] Whittaker T, Collier D, Folley M, Osterried M, Henry A, Crowley M. The development of oyster—a shallow water surging wave energy converter. In: Proceedings of the 7th European wave and tidal energy conference. 2007, p. 11–4.

[41] Hansen RH, Kramer MM, Vidal E. Discrete displacement hydraulic power take-off system for the wavestar wave energy converter. Energies 2013;6(8):4001–44.

[42] Vakis AI, Anagnostopoulos JS. Mechanical design and modeling of a single-piston pump for the novel power take-off system of a wave energy converter. Renewable Energy 2016;96:531–47.

[43] Wei Y, Barradas-Berglind J, Van Rooij M, Prins W, Jayawardhana B, Vakis A. Investigating the adaptability of the multi-pump multi-piston power take-off system for a novel wave energy converter. Renewable Energy 2017;111:598–610.

[44] Albert A, Berselli G, Bruzzone L, Fanghella P. Mechanical design and simulation of an onshore four-bar wave energy converter. Renewable Energy 2017;114:766–74.

[45] Shadman M, Avalos GOG, Estefen SF. On the power performance of a wave energy converter with a direct mechanical drive power take-off system controlled by latching. Renewable Energy 2021;169:157–77.

[46] Eriksson M, Isberg J, Leijon M. Hydrodynamic modelling of a direct drive wave energy converter. International Journal of Engineering Science 2005;43(17-18):1377–87.

[47] Leijon M, Danielsson O, Eriksson M, Thorburn K, Bernhoff H, Isberg J, et al. An electrical approach to wave energy conversion. Renewable energy 2006;31(9):1309–19.

[48] Prudell J, Stoddard M, Amon E, Brekken TK, Von Jouanne A. A permanent-magnet tubular linear generator for ocean wave energy conversion. IEEE Transactions on Industry Applications 2010;46(6):2392–400.

[49] Platts M. Engineering development of the lancaster flexible bag. Tech. Rep.; Wavepower Limited; 1981.

[50] Bellamy N. An alternative design of the sea clam wave energy converter. In: Proc. of the ASME Fourth International Offshore Mechanics and Arctic Engineering Symposium; vol. 1. 1985,.

[51] Rohrer JW. Ocean wave energy converter with multiple capture modes. U.S. Patent 8,604,631, Dec 10, 2013.

[52] French M. Conceptual design for engineers. Springer; 1985.

[53] Brooke J. Wave energy conversion; vol. 6. Elsevier; 2003.

[54] Huang M, Aggidis G. Developments, expectations of wave energy converters and mooring anchors in the uk. Journal of Ocean University of China 2008;7(1):10–6.

[55] Bellamy N. Development of the sea clam wave energy converter. In: Proc. 2nd Int. Symp. on Wave Energy Utilization, Trondheim, Norway; vol. 22. 1982, p. 24.

[56] Bellamy N, Peatfield A. Further development of the sea clam wave energy converter. In: the IEE Fourth International Conference on Energy Options, London. 1984,.

[57] Peatfield A, Bellamy N, Duckers L, Lockett F, Loughbridge B, West M, et al. Wave energy: a british way forward with the circular sea-clam. Energy Options 1987;:194.

[58] Bucchi A, Hearn G. Analysis of the sea-owc-clam wave energy device part b: Structural integrity analysis. Renewable energy 2016;99:253–69.

[59] Bellamy N, Bucchi A, Hearn G. Analysis of the sea-owc-clam wave energy device–part a: Historical development, hydrodynamic and motion response formulations & solutions. Renewable energy 2016;88:220–35.

[60] Turner DM. Energy conversion device. U.S. Patent Application 12/992,697, Aug 4, 2011.

[61] Technology Description and Status AWS-III. Tech. Rep.; AWS and Wave Energy Scotland; 2016.

[62] AWS, Research and Development. https://www.awsocean.com/research-development/; 2020 [Accessed 29 May 2021].

[63] 4c Engineering, AWS – Technology Demonstrator. Available at https://www.4cengineering.co.uk/case-studies/aws-ocean-energy-technology-demonstrator; 2020 [Accessed 28 October 2020].

[64] Leighton S, Algie C, Ryan SK. Wave energy conversion/convertors. U.S. Patent 10,883,471, Jan 5, 2021.

[65] Ryan GL, Ryan SK. Wave energy conversion. U.S. Patent 9,797,367, Oct 24, 2017.

[66] Orphin J, Fleming A, Algie C. Physical scale model testing of a flexible membrane wave energy converter: Videogrammetric analysis of membrane operation. International journal of marine energy 2017;20:135–50.

[67] Algie C, Fleming A, Ryan S. Experimental and numerical modelling of the bombora wave energy converter. In: 3rd Asian Wave and Tidal Energy Conference (AWTEC 2016); vol. 2. 2016, p. 719–25.

[68] Algie C, Ryan S, Fleming A. Predicted power performance of a submerged membrane pressure-differential wave energy converter. International journal of marine energy 2017;20:125–34.

[69] Bombora, About the Pembrokeshire project. https://bomborawave.com/latest-news/project/1-5mw-pembrokeshire-project/; 2020 [Accessed 29 May 2021].

[70] Bombora prepares for Portugal Wave Farm after Strong LCOE Results. Tech. Rep.; Bombora Wave Power; 2016.

[71] Bombora Wave Power. Bombora prepares for Portugal Wave Farm after Strong LCOE Results. Tech. Rep.; Bombora Wave Power; 2016.

[72] McNatt J, Özkan-Haller H, Delos-Reyes M. Preliminary modeling and analysis of a horizontal pressure differential wave energy converter. Journal of Offshore Mechanics and Arctic Engineering 2014;136(1).

[73] Babarit A, Wendt F, Yu Y, Weber J. Investigation on the energy absorption performance of a fixed-bottom pressure-differential wave energy converter. Applied Ocean Research 2017;65:90–101.

[74] Offshore Energy, Video: M3 Wave's DMP wave energy converter. https://www.offshore-energy.biz/video-m3-waves-dmp-wave-energy-converter; 2020 [28 October 2020].

[75] Yu YH. M3 wave system modeling: Cooperative research and development final report, crada number crd-17-697. Tech. Rep.; National Renewable Energy Lab.(NREL), Golden, CO (United States); 2019.

[76] Kurniawan A, Chaplin J, Greaves D, Hann M. Wave energy absorption by a floating air bag. Journal of Fluid Mechanics 2017;812:294–320.

[77] Kurniawan A, Chaplin J, Hann M, Greaves D, Farley F. Wave energy absorption by a submerged air bag connected to a rigid float. Proceedings of the Royal Society A: Mathematical, Physical and Engineering Sciences 2017;473(2200):20160861.

[78] Kurniawan A, Greaves D. Wave power absorption by a submerged balloon fixed to the sea bed. IET Renewable Power Generation 2016;10(10):1461–7.

[79] Greaves D, Hann M, Kurniawan A, Chaplin J, Farley F. The hydrodynamics of air-filled bags for wave energy conversion. In: International Conference on Offshore Renewable Energy. 2016,.

[80] Fontana M, Daniele L, Moretti G. Damiani D, Righi M, Vertechy R, Teillant B, et al. Wave motion generator based on a dielectric elastomer with stiffness compensation. WO Patent 2018/116276, Jun 28, 2018.

[81] Farley F, Rainey R, Chaplin J. Rubber tubes in the sea. Philosophical Transactions of the Royal Society A: Mathematical, Physical and Engineering Sciences 2012;370(1959):381–402.

[82] Lighthill J. Waves in fluids. Cambridge university press; 1978.

[83] Farley FJM, Rainey RCT. Distensible tube wave energy converter. U.S. 7,980,071, 2011 Jul 19.

[84] WES Novel Wave Energy Converter, Stage 1 Project, Project Report. Tech. Rep.; Checkmate Seaenergy and Wave Energy Scotland; 2017.

[85] Hann M, Chaplin J, Farley F. Assessment of a multi-cell fabric structure as an attenuating wave energy converter. In: World Renewable Energy Congress-Sweden; 8-13 May; 2011; Linköping; Sweden. 057; Linköping University Electronic Press; 2011, p. 2143–50.

[86] Chaplin J, Heller V, Farley F, Hearn G, Rainey R. Laboratory testing the anaconda. Philosophical Transactions of the Royal Society A: Mathematical, Physical and Engineering Sciences 2012;370(1959):403–24.

[87] Mendes A, Paredes L, Gil F, Chaplin J. Small-scale model tests of a rubber-tube wave energy converter with pneumatic power take-off. In: ASME 2014 33rd International Conference on Ocean, Offshore and Arctic Engineering. 2014,.

[88] Mendes A, Braga F, Paredes L, Chaplin J. Performance assessment of the anaconda wec in regular waves at 1: 50 model scale. In: ASME 2017 36th International Conference on Ocean, Offshore and Arctic Engineering. 2017,.

[89] Sea Energy Anaconda. Available at https://www.checkmateukseaenergy.com/; 2020 [28 October 2020].

[90] Pollack J, Jean PF. Wave energy converter. U.S. Patent 8,120,195, Feb 21, 2012.

[91] Jean P, Wattez A, Ardoise G, Melis C, Van Kessel R, Fourmon A, et al. Standing wave tube electro active polymer wave energy converter. In: Electroactive Polymer Actuators and Devices (EAPAD) 2012; vol. 8340. International Society for Optics and Photonics; 2012, p. 83400C.

[92] Grey S, Borthwick A. Apparatus and method for extracting energy from fluid motion. U.S. Patent 8,633,6082014, Jan 21, 2014.

[93] Technology Description and Status Electric Eel. Tech. Rep.; AWS and Wave Energy Scotland; 2016.

[94] Andritsch T, Morshuis P, Smit J, Jean P, van Kessel R, Wattez A, et al. Challenges of using electroactive polymers in large scale wave energy converters. In: 2012 Annual Report Conference on Electrical Insulation and Dielectric Phenomena. 2012, p. 786–9.

[95] SBM Offshore, SBM Offshore Technology Wave Energy Converter. Available at https://www.sbmoffshore.com/wp-content/uploads/2019/11/SBM-Offshore_Technology_Wave-Energy-Converter.pdf; 2020 [Accesed 28 October 2020].

[96] Babarit A, Singh J, Mélis C, Wattez A, Jean P. A linear numerical model for analysing the hydroelastic response of a flexible electroactive wave energy converter. Journal of Fluids and Structures 2017;74:356–84.

[97] Wattez A. The Future of WEC is Flexible with Distributed PTO; 2018. Presented at ICOE 2018 International Conference On Ocean Energy, Cherbourg, Normandy, France.

[98] SBM Offshore, Sea trial in the Principality of Monaco announced for SBM Offshore's innovative S3 Wave Energy Converter. https://www.sbmoffshore.com/news/sea-trial-in-the-principality-of-monaco-announced-for-sbm-offshores-innovative-s3-wave-energy-converter/; 2020 [Accessed 28 October 2020].

[99] AWS, Electric Eel Flexible Wave Power Attenuator. https://www.awsocean.com/flexible-wave-power/; 2020 [Accessed 28 October 2020].

[100] Energy island, wave energy conversion. http://www.energyisland.com/projects/lilypad/lilypad.html; 2020 [Accessed 28 October 2020].

[101] Solar energy limited, biography. http://http://www.solarenergyltd.net/; 2020 [Accessed 28 October 2020].

[102] Alam Mr, Lehmann M, Shakeri M. Carpet of wave energy conversion (cwec). U.S. Patent 9,777,701, Oct 3, 2017.

[103] Lehmann M, Elandt R, Shakeri M, Alam R. The wave carpet: development of a submerged pressure differential wave energy converter. In: 30th Symposium on Naval Hydrodynamics. 2014, p. 2–7.

[104] Alam M. Nonlinear analysis of an actuated seafloor-mounted carpet for a high-performance wave energy extraction. Proceedings of the Royal Society A: Mathematical, Physical and Engineering Sciences 2012;468(2146):3153–71.

[105] Marine and Hydrokinetic Data Repository, CalWave Device Behavior in Different Sea States from Scaled Tank Testing. https://mhkdr.openei.org/submissions/250; 2020 [Accessed 28 October 2020].

[106] Taylor G, Burns J, Kammann S, Powers W, Welsh T. The energy harvesting eel: a small subsurface ocean/river power generator. IEEE journal of oceanic engineering 2001;26(4):539–47.

[107] Techet A, Allen J, Smits A, et al. Piezoelectric eels for energy harvesting in the ocean. In: The Twelfth International Offshore and Polar Engineering Conference. 2002,.

[108] Yin G, Yang Y, Song F, Renard C, Dang Z, Shi C, et al. Dielectric elastomer generator with improved energy density and conversion efficiency based on polyurethane composites. ACS applied materials & interfaces 2017;9(6):5237–43.

[109] Cao J, E S, Guo Z, Gao Z, Luo H. Electromechanical conversion efficiency for dielectric elastomer generator in different energy harvesting cycles. AIP Advances 2017;7(11):115117.

[110] Lai Z, Thomson G, Yurchenko D, Val DV, Rodgers E. On energy harvesting from a vibro-impact oscillator with dielectric membranes. Mechanical Systems and Signal Processing 2018;107:105–21.

[111] Thomson G, Lai Z, Val DV, Yurchenko D. Advantages of nonlinear energy harvesting with dielectric elastomers. Journal of Sound and Vibration 2019;442:167–82.

[112] Moretti G, Rosati P. GP, Daniele L, Forehand D, Ingram D, Vertechy R, et al. Modelling and testing of a wave energy converter based on dielectric elastomer generators. Proceedings of the Royal Society A 2019;475(2222):20180566.

[113] Kornbluh RD, Pelrine R, Prahlad H, Wong-Foy A, McCoy B, Kim S, et al. From boots to buoys: promises and challenges of dielectric elastomer energy harvesting. In: Electroactivity in polymeric materials. Springer; 2012, p. 67–93.

[114] Scherber B, Grauer M, Köllnberger A. Electroactive polymers for gaining sea power. In: Bar-Cohen Y, editor. Electroactive Polymer Actuators and Devices (EAPAD) 2013; vol. 8687. International Society for Optics and Photonics; SPIE; 2013, p. 149 –55.

[115] Hydropower, Electroactive Polymers (EAPs) for Energy Generation. https://www.wacker.com/cms/en-us/products/applications/renewable-energies/hydropower/hydropower.html; 2020 [Accessed 28 October 2020].

[116] Moretti G, Fontana M, Vertechy R. Modeling of a heaving buoy wave energy converter with stacked dielectric elastomer generator. In: ASME 2014 Conference on Smart Materials, Adaptive Structures and Intelligent Systems. 2014,.

[117] Whittaker T, Folley M. Nearshore oscillating wave surge converters and the development of oyster. Philosophical Transactions of the Royal Society A: Mathematical, Physical and Engineering Sciences 2012;370(1959):345–64.

[118] Wille H, Boureau S. Near Shore WEC System. WO Patent 2011/151693, Dec 8, 2011.

[119] Moretti G, Fontana M, Vertechy R. Modeling and control of lozenge-shaped dielectric elastomer generators. In: ASME 2013 Conference on Smart Materials, Adaptive Structures and Intelligent Systems. 2013,.

[120] Moretti G, Forehand D, Vertechy R, Fontana M, Ingram D. Modeling of an oscillating wave surge converter with dielectric elastomer power take-off. In: ASME 2014 33rd International Conference on Ocean, Offshore and Arctic Engineering. 2014,.

[121] Moretti G, Malara G, Scialò A, Daniele L, Romolo A, Vertechy R, et al. Modelling and field testing of a breakwater-integrated u-owc wave energy converter with dielectric elastomer generator. Renewable Energy 2020;146:628–42.

[122] Symphony Wave Power, How does it work? https://symphonywavepower.com/how-does-it-work/; 2020 [Accessed 28 October 2020].

[123] Quoceant . Marine automatically stowable and inflatable volume. Tech. Rep.; Quoceant and Wave Energy Scotland; 2017.

[124] Kent Online, Anaconda wave energy technology developer Checkmate Seaenergy in Sheerness awarded cash from Scottish government scheme. https://www.kentonline.co.uk/kent-business/county-news/anaconda-wave-energy-technology-made-by-checkmate-seaenergy-sheerness-awarded-cash-scottish-government-scheme-130930/; 2020 [Accessed 28 October 2020].

[125] Sea Energy Associates Ltd, The Sea Clam. http://www.seaclam.co.uk/the_sea_clam_technology.html; 2020 [Accessed 28 October 2020].

[126] Diani J, Fayolle B, Gilormini P. A review on the mullins effect. European Polymer Journal 2009;45(3):601–12.

[127] Kornbluh R, Pelrine R, Prahlad H, Wong-Foy A, McCoy B, Kim S, et al. Dielectric elastomers: Stretching the capabilities of energy harvesting. MRS bulletin 2012;37(3):246.

[128] Biggs J, Danielmeier K, Hitzbleck J, Krause J, Kridl T, Nowak S, et al. Electroactive polymers: developments of and perspectives for dielectric elastomers. Angewandte Chemie International Edition 2013;52(36):9409–21.

[129] Le Gac PY, Le Saux V, Paris M, Marco Y. Ageing mechanism and mechanical degradation behaviour of polychloroprene rubber in a marine environment: Comparison of accelerated ageing and long term exposure. Polymer degradation and stability 2012;97(3):288–96.

[130] Davies P, Le Gac PY, Le Gall M, Arhant M, Humeau C. Durability of polymers and composites: The key to reliable marine renewable energy production. In: ASME 2018 37th International Conference on Ocean, Offshore and Arctic Engineering. American Society of Mechanical Engineers Digital Collection; 2018,.

[131] Mars W, Fatemi A. Factors that affect the fatigue life of rubber: a literature survey. Rubber Chemistry and Technology 2004;77(3):391–412.

[132] Tee YL, Loo MS, Andriyana A. Recent advances on fatigue of rubber after the literature survey by mars and fatemi in 2002 and 2004. International Journal of Fatigue 2018;110:115–29.

[133] Roberts B, Benzies J. The relationship between uniaxial and equibiaxial fatigue in gum and carbon black filled vulcanizates. Proceedings of rubbercon 1977;77(2):1–13.

[134] Roach JF. Crack growth in elastomers under biaxial stresses: A dissertation presented to the graduate faculty of the university of akron. Ph.D. thesis; 1982.

[135] Cadwell S, Merrill R, Sloman C, Yost F. Dynamic fatigue life of rubber. Industrial & Engineering Chemistry Analytical Edition 1940;12(1):19–23.

[136] Abraham F, Alshuth T, Jerrams S. The effect of minimum stress and stress amplitude on the fatigue life of non strain crystallising elastomers. Materials & Design 2005;26(3):239–45.

[137] Riaya A, Shaw MT, Garton A. Oxidation of elastomers in aqueous environments. Rubber chemistry and technology 1994;67(5):775–85.

[138] Le Gac PY. Durability of polychloroprene rubber for marine application. Ph.D. thesis; Paris, ENSAM; 2014.

[139] Davies P, Evrard G. Accelerated ageing of polyurethanes for marine applications. Polymer Degradation and Stability 2007;92(8):1455–64.

[140] Rabanizada N, Lupberger F, Johlitz M, Lion A. Experimental investigation of the dynamic mechanical behaviour of chemically aged elastomers. Archive of Applied Mechanics 2015;85(8):1011–23.

[141] Selden R. The effect of water immersion on fatigue crack growth of two engineering rubbers. Journal of applied polymer science 1998;69(5):941–6.

[142] Mott P, Roland C. Aging of natural rubber in air and seawater. Rubber chemistry and technology 2001;74(1):79–88.

[143] Le Gac PY, Arhant M, Davies P, Muhr A. Fatigue behavior of natural rubber in marine environment: Comparison between air and sea water. Materials & Design (1980-2015) 2015;65:462–7.

[144] Ulu KN, Huneau B, Le Gac PY, Verron E. Fatigue resistance of natural rubber in seawater with comparison to air. International Journal of Fatigue 2016;88:247–56.

[145] Kornbluh R, Wong-Foy A, Pelrine R, Prahlad H, McCoy B. Long-lifetime all-polymer artificial muscle transducers. MRS Online Proceedings Library Archive 2010;1271.

[146] Yi C, Agostini L, Fontana M, Moretti G, Vertechy R. On the lifetime performance of a styrenic rubber membrane for dielectric elastomer transducers. In: Smart Materials, Adaptive Structures and Intelligent Systems; vol. 51944. American Society of Mechanical Engineers; 2018, p. V001T03A028.

[147] de Saint-Aubin CA, Rosset S, Schlatter S, Shea H. High-cycle electromechanical aging of dielectric elastomer actuators with carbon-based electrodes. Smart Materials and Structures 2018;27(7):074002.

[148] Jean-Mistral C, Jacquet-Richardet G, Sylvestre A. Parameters influencing fatigue life prediction of dielectric elastomer generators. Polymer Testing 2020;81:106198.

[149] Patil A. Inflation and instabilities of hyperelastic membranes. Ph.D. thesis; KTH Royal Institute of Technology; 2016.

[150] Patil A, DasGupta A. Finite inflation of an initially stretched hyperelastic circular membrane. European Journal of Mechanics-A/Solids 2013;41:28–36.

[151] Patil A, Nordmark A, Eriksson A. Free and constrained inflation of a pre-stretched cylindrical membrane. Proceedings of the Royal Society A: Mathematical, Physical and Engineering Sciences 2014;470(2169):20140282.

[152] Patil A, Nordmark A, Eriksson A. Instability investigation on fluid-loaded pre-stretched cylindrical membranes. Proceedings of the Royal Society A: Mathematical, Physical and Engineering Sciences 2015;471(2177):20150016.

[153] Haughton D, Ogden R. Bifurcation of inflated circular cylinders of elastic material under axial loading—i. membrane theory for thin-walled tubes. Journal of the Mechanics and Physics of Solids 1979;27(3):179–212.

[154] Alexander H. The tensile instability of an inflated cylindrical membrane as affected by an axial load. International Journal of Mechanical Sciences 1971;13(2):87–95.

[155] Kanner LM, Horgan CO. Elastic instabilities for strain-stiffening rubber-like spherical and cylindrical thin shells under inflation. International Journal of Non-Linear Mechanics 2007;42(2):204–15.

[156] Bucchi A, Hearn G. Delay or removal of aneurysm formation in the anaconda wave energy extraction device. Renewable energy 2013;55:104–19.

[157] Dorfmann L, Ogden RW. Nonlinear electroelasticity: material properties, continuum theory and applications. Proceedings of the Royal Society A: Mathematical, Physical and Engineering Sciences 2017;473(2204):20170311.

[158] Zhao X, Sharma P. Avoiding the pull-in instability of a dielectric elastomer film and the potential for increased actuation and energy harvesting. Soft Matter 2017;13(26):4552–8.

[159] Su Y, Chen W, Destrade M. Tuning the pull-in instability of soft dielectric elastomers through loading protocols. International Journal of Non-Linear Mechanics 2019;113:62–6.

[160] Sharma AK, Arora N, Joglekar M. Dc dynamic pull-in instability of a dielectric elastomer balloon: an energy-based approach. Proceedings of the Royal Society A: Mathematical, Physical and Engineering Sciences 2018;474(2211):20170900.

[161] Chen Y, Agostini L, Moretti G, Fontana M, Vertechy R. Dielectric elastomer materials for large-strain actuation and energy harvesting: a comparison between styrenic rubber, natural rubber and acrylic elastomer. Smart Materials and Structures 2019;28(11):114001.

[162] Li T, Qu S, Yang W. Energy harvesting of dielectric elastomer generators concerning inhomogeneous fields and viscoelastic deformation. Journal of Applied Physics 2012;112(3):034119.

[163] Hossain M, Liao Z. An additively manufactured silicone polymer: Thermo-viscoelastic experimental study and computational modelling. Additive Manufacturing 2020;:101395.

[164] Parida K, Kumar V, Jiangxin W, Bhavanasi V, Bendi R, Lee PS. Highly transparent, stretchable, and self-healing ionic-skin triboelectric nanogenerators for energy harvesting and touch applications. Advanced Materials 2017;29(37):1702181.

[165] Vu-Cong T, Jean-Mistral C, Sylvestre A. Impact of the nature of the compliant electrodes on the dielectric constant of acrylic and silicone electroactive polymers. Smart Materials and Structures 2012;21(10):105036.

[166] O'Bryan CS, Bhattacharjee T, Hart S, Kabb CP, Schulze KD, Chilakala I, et al. Self-assembled micro-organogels for 3d printing silicone structures. Science advances 2017;3(5):e1602800.

[167] Zhou Ly, Gao Q, Fu Jz, Chen Qy, Zhu Jp, Sun Y, et al. Multimaterial 3d printing of highly stretchable silicone elastomers. ACS applied materials & interfaces 2019;11(26):23573–83.

[168] Ruellan B, Le Cam JB, Jeanneau I, Canévet F, Mortier F, Robin E. Fatigue of natural rubber under different temperatures. International Journal of Fatigue 2019;124:544–57.

[169] Moretti G, Papini G, Righi M, Forehand D, Ingram D, Vertechy R, et al. Resonant wave energy harvester based on dielectric elastomer generator. Smart Materials and Structures 2018;27(3):035015.

[170] Liao Z, Hossain M, Yao X, Mehnert M, Steinmann P. On thermo-viscoelastic experimental characterization and numerical modelling of vhb polymer. International Journal of Non-Linear Mechanics 2020;118:103263.

[171] Fröhlich J, Niedermeier W, Luginsland H. The effect of filler–filler and filler–elastomer interaction on rubber reinforcement. Composites Part A: Applied Science and Manufacturing 2005;36(4):449–60.

[172] Kumar A, Patra K, Hossain M. Silicone composites cured under a high electric field: An electromechanical experimental study. Polymer Composites 2021;42(2):914–30.

[173] Kumar A, Ahmad D, Patra K, Hossain M. Enhancement of electromechanical properties of natural rubber by adding barium titanate filler: An electro-mechanical study. Journal of Applied Polymer Science 2021;0(0):00–.

[174] Zhang S, Zheng L, Liu D, Xu Z, Zhang L, Liu L, et al. Improved mechanical and fatigue properties of graphene oxide/silica/sbr composites. RSC Advances 2017;7:40813.

[175] Wei L, Fu X, Luo M, Xie Z, Huang C, Zhou J, et al. Synergistic effect of cb and go/cnt hybrid fillers on the mechanical properties and fatigue behavior of nr composites. RSC Advances 2018;8:10573.

[176] Mollica RR, Sweet HT. Method of making inflatable fabric lined rubber articles. US Patent 2689812, Sep 21, 1954.

[177] Duckers L, et al. Reinforced rubber membranes for the clam wave energy converter. In: The Ninth International Offshore and Polar Engineering Conference. International Society of Offshore and Polar Engineers; 1999,.

[178] Kovacs G, Düring L, Michel S, Terrasi G. Stacked dielectric elastomer actuator for tensile force transmission. Sensors and actuators A: Physical 2009;155(2):299–307.

[179] McKay T, O'Brien B, Calius E, Anderson I. Self-priming dielectric elastomer generators. Smart Materials and Structures 2010;19(5):055025.

[180] Rosset S, Shea H. Flexible and stretchable electrodes for dielectric elastomer actuators. Applied Physics A 2013;110(2):281–307.

[181] Verplancke R, Bossuyt F, Cuypers D, Vanfleteren J. Thin-film stretchable electronics technology based on meandering interconnections: fabrication and mechanical performance. Journal of Micromechanics and Microengineering 2011;22(1):015002.

[182] Bowden N, Brittain S, Evans AG, Hutchinson JW, Whitesides GM. Spontaneous formation of ordered structures in thin films of metals supported on an elastomeric polymer. Nature 1998;393(6681):146–9.

[183] Benslimane M, Gravesen P, Sommer-Larsen P. Mechanical properties of dielectric elastomer actuators with smart metallic compliant electrodes. In: Smart Structures and Materials 2002: Electroactive polymer actuators and devices (EAPAD); vol. 4695. 2002, p. 150–7.

[184] Cruz J. Ocean wave energy: current status and future prespectives. Springer Science & Business Media; 2007.

[185] Ruehl K, Michelen C, Kanner S, Lawson M, Yu YH. Preliminary verification and validation of wec-sim, an open-source wave energy converter design tool. In: International Conference on Offshore Mechanics and Arctic Engineering; vol. 45547. American Society of Mechanical Engineers; 2014, p. V09BT09A040.

[186] Palm J, Eskilsson C, Paredes GM, Bergdahl L. Coupled mooring analysis for floating wave energy converters using cfd: Formulation and validation. International Journal of Marine Energy 2016;16:83–99.

[187] Ransley E, Greaves D, Raby A, Simmonds D, Hann M. Survivability of wave energy converters using cfd. Renewable Energy 2017;109:235–47.

[188] Steinmann P, Hossain M, Possart G. Hyperelastic models for rubber-like materials: consistent tangent operators and suitability for treloar's data. Archive of Applied Mechanics 2012;82(9):1183–217.

[189] Hossain M, Steinmann P. More hyperelastic models for rubber-like materials: consistent tangent operators and comparative study. Journal of the Mechanical Behavior of Materials 2013;22(1-2):27–50.

[190] Hossain M, Amin A, Kabir MN. Eight-chain and full-network models and their modified versions for rubber hyperelasticity: a comparative study. Journal of the Mechanical Behavior of Materials 2015;24(1-2):11–24.

[191] Carroll M. A strain energy function for vulcanized rubbers. Journal of Elasticity 2011;103(2):173–87.

[192] Hossain M, Vu DK, Steinmann P. Experimental study and numerical modelling of vhb 4910 polymer. Computational Materials Science 2012;59:65–74.

[193] Linder C, Tkachuk M, Miehe C. A micromechanically motivated diffusion-based transient network model and its incorporation into finite rubber viscoelasticity. Journal of the Mechanics and Physics of Solids 2011;59(10):2134–56.

[194] Saxena P, Hossain M, Steinmann P. A theory of finite deformation magneto-viscoelasticity. International Journal of Solids and Structures 2013;50(24):3886–97.

[195] Reese S, Govindjee S. A theory of finite viscoelasticity and numerical aspects. International journal of solids and structures 1998;35(26-27):3455–82.

[196] Liao Z, Hossain M, Yao X, Mehnert M, Steinmann P. On thermo-viscoelastic experimental characterization and numerical modelling of vhb polymer. International Journal of Non-Linear Mechanics 2020;118:103263.

[197] Lubliner J. A model of rubber viscoelasticity. Mechanics Research Communications 1985;12(2):93–9.

[198] Amin A, Lion A, Sekita S, Okui Y. Nonlinear dependence of viscosity in modeling the rate-dependent response of natural and high damping rubbers in compression and shear: Experimental identification and numerical verification. International Journal of Plasticity 2006;22(9):1610–57.

[199] Johlitz M, Diercks N, Lion A. Thermo-oxidative ageing of elastomers: A modelling approach based on a finite strain theory. International Journal of Plasticity 2014;63:138–51.

[200] Lion A, Johlitz M. On the representation of chemical ageing of rubber in continuum mechanics. International Journal of Solids and Structures 2012;49(10):1227–40.

[201] de Souza Neto E, Perić D, Owen D. Continuum modelling and numerical simulation of material damage at finite strains. Archives of Computational Methods in Engineering 1998;5(4):311.

[202] Ayoub G, Naït-Abdelaziz M, Zaïri F, Gloaguen JM, Charrier P. A continuum damage model for the high-cycle fatigue life prediction of styrene-butadiene rubber under multiaxial loading. International Journal of Solids and Structures 2011;48(18):2458–66.

[203] Jha NK, Nackenhorst U, Pawar VS, Nadella R, Guruprasad P. On the constitutive modelling of fatigue damage in rubber-like materials. International Journal of Solids and Structures 2019;159:77–89.

[204] Mohammadi H, Dargazany R. Micro-mechanical model for thermo-oxidative aging of elastomers. In: ASME International Mechanical Engineering Congress and Exposition; vol. 52149. American Society of Mechanical Engineers; 2018, p. V009T12A028.

[205] Bahrololoumi A, Mohammadi H, Moravati V, Dargazany R. A physically-based model for thermo-oxidative and hydrolytic aging of elastomers. International Journal of Mechanical Sciences 2021;194:106193.

[206] Mehnert M, Hossain M, Steinmann P. Numerical modeling of thermo-electro-viscoelasticity with field-dependent material parameters. International Journal of Non-Linear Mechanics 2018;106:13–24.

[207] Vertechy R, Papini Rosati GP, Fontana M. Reduced model and application of inflating circular diaphragm dielectric elastomer generators for wave energy harvesting. Journal of Vibration and Acoustics 2015;137(1).

[208] Babarit A, Singh J, Mélis C, Wattez A, Jean P. A linear numerical model for analysing the hydroelastic response of a flexible electroactive wave energy converter. Journal of Fluids and Structures 2017;74:356–84.

[209] Causin P, Gerbeau JF, Nobile F. Added-mass effect in the design of partitioned algorithms for fluid–structure problems. Computer methods in applied mechanics and engineering 2005;194(42-44):4506–27.

[210] Ransley EJ, Brown SA, Hann M, Greaves DM, Windt C, Ringwood J, et al. Focused wave interactions with floating structures: A blind comparative study. Proceedings of the Institution of Civil Engineers-Engineering and Computational Mechanics 2021;174(1):46–61.

[211] Renzi E, Dias F. Hydrodynamics of the oscillating wave surge converter in the open ocean. European Journal of Mechanics-B/Fluids 2013;41:1–10.

[212] Dafnakis E, Dias F. Comparison of wave-structure interaction dynamics of a submerged cylindrical point absorber with three degrees of freedom using potential flow and cfd models. Prepreint 2020;.

[213] Lee CH. WAMIT theory manual. Massachusetts Institute of Technology, Department of Ocean Engineering; 1995.

[214] Babarit A, Delhommeau G. Theoretical and numerical aspects of the open source bem solver nemoh. 2015,.

[215] Selby JC, Shannon MA. Inflation of a circular elastomeric membrane into a horizontally semi-infinite liquid reservoir of finite vertical depth: Quasi-static deformation model. International journal of engineering science 2009;47(5-6):700–17.

[216] Eriksson A, Nordmark A, Patil A, Zhou Y. Parametric stability investigations for hydrostatically loaded membranes. Computers & Structures 2016;174:33–41.

[217] Bonet J, Wood R, Mahaney J, Heywood P. Finite element analysis of air supported membrane structures. Computer methods in applied mechanics and engineering 2000;190(5-7):579–95.

[218] Verron E, Marckmann G, Peseux B. Dynamic inflation of non-linear elastic and viscoelastic rubber-like membranes. International Journal for Numerical Methods in Engineering 2001;50(5):1233–51.

[219] Coelho M, Roehl D, Bletzinger KU. Numerical and analytical solutions with finite strains for circular inflated membranes considering pressure–volume coupling. International Journal of Mechanical Sciences 2014;82:122–30.

[220] Algie C, Ryan S, Fleming A. Predicted power performance of a submerged membrane pressure-differential wave energy converter. International journal of marine energy 2017;20:125–34.

[221] Formaggia L, Lamponi D, Quarteroni A. One-dimensional models for blood flow in arteries. Journal of engineering mathematics 2003;47(3-4):251–76.

[222] Chaplin J, Farley F, Greaves D, Hann M, Kurniawan A, Cox M. Numerical and experimental investigation of wave energy devices with inflated bags. In: Proceedings of 11th European Wave and Tidal Energy Conference, Nantes, France. 2015,.

[223] Chaplin J, Farley F, Kurniawan A, Greaves D, Hann M. Forced heaving motion of a floating air-filled bag. In: Proc. 30th Int. Workshop on Water Waves and Floating Bodies. Bristol, UK. 2015,.

[224] Newman JN. Wave effects on deformable bodies. Applied ocean research 1994;16(1):47–59.

[225] McDonald A, Xiao Q, Forehand D, Smith H, Costello R. Initial development of a generic method for analysis of flexible membrane wave energy converters. In: Advances in Renewable Energies Offshore: Proceedings of the 3rd International Conference on Renewable Energies Offshore (RENEW 2018), October 8-10, 2018, Lisbon, Portugal. CRC Press; 2018, p. 333.

[226] McDonald A, Xiao Q, Forehand D, Costello R. Linear analysis of fluid-filled membrane structures using generalised modes. In: Proceedings of the 13th European Wave and Tidal Energy Conference. 2019,.

[227] Guo Y, Yu YH, van Rij JA, Tom NM. Inclusion of structural flexibility in design load analysis for wave energy converters. Tech. Rep.; National Renewable Energy Lab.(NREL), Golden, CO (United States); 2017.

[228] Ancellin M, Dong M, Jean P, Dias F. Far-field maximal power absorption of a bulging cylindrical wave energy converter. Energies 2020;13(20):5499.

[229] Dettmer W, Perić D. A computational framework for fluid–structure interaction: finite element formulation and applications. Computer Methods in Applied Mechanics and Engineering 2006;195(41-43):5754–79.

[230] Bazilevs Y, Takizawa K, Tezduyar TE. Computational fluid-structure interaction: methods and applications. John Wiley & Sons; 2013.

[231] Zienkiewicz OC, Taylor RL, Nithiarasu P. The finite element method for fluid dynamics; vol. 6. Elsevier; 2015.

[232] King A, Algie C, Ryan S, Ong R. Modelling of fluid structure interactions in submerged flexible membranes for the bombora wave energy converter. In: 20th Australasian Fluid Mechanics Conference, Perth, Australia. 2016,.

[233] Ryzhakov PB, Oñate E. A finite element model for fluid–structure interaction problems involving closed membranes, internal and external fluids. Computer Methods in Applied Mechanics and Engineering 2017;326:422–45.

[234] Burman E, Claus S, Hansbo P, Larson MG, Massing A. Cutfem: discretizing geometry and partial differential equations. International Journal for Numerical Methods in Engineering 2015;104(7):472–501.

[235] Dettmer W, Kadapa C, Perić D. A stabilised immersed boundary method on hierarchical b-spline grids. Computer Methods in Applied Mechanics and Engineering 2016;311:415–37.

[236] Kadapa C, Dettmer W, Perić D. A stabilised immersed framework on hierarchical b-spline grids for fluid-flexible structure interaction with solid–solid contact. Computer Methods in Applied Mechanics and Engineering 2018;335:472–89.

[237] Hughes TJ. Linear static and dynamic finite element analysis. The Finite Element Method, Prentice-Hall, Inc 1987;.

[238] Zienkiewicz OC, Taylor RL. The finite element method for solid and structural mechanics. Elsevier; 2013.

[239] Dettmer WG, Lovrić A, Kadapa C, Perić D. New iterative and staggered solution schemes for incompressible fluid-structure interaction based on dirichlet-neumann coupling. International Journal for Numerical Methods in Engineering 2020;.

[240] Fernández MA, Mullaert J, Vidrascu M. Generalized robin–neumann explicit coupling schemes for incompressible fluid-structure interaction: Stability analysis and numerics. International Journal for Numerical Methods in Engineering 2015;101(3):199–229.

[241] Burman E, Fernández MA. An unfitted nitsche method for incompressible fluid–structure interaction using overlapping meshes. Computer Methods in Applied Mechanics and Engineering 2014;279:497–514.

[242] Boilevin-Kayl L, Fernández MA, Gerbeau JF. A loosely coupled scheme for fictitious domain approximations of fluid-structure interaction problems with immersed thin-walled structures. SIAM Journal on Scientific Computing 2019;41(2):B351–74.

[243] Dettmer WG, Perić D. A new staggered scheme for fluid–structure interaction. International Journal for Numerical Methods in Engineering 2013;93(1):1–22.

[244] Farhat C, Rallu A, Wang K, Belytschko T. Robust and provably second-order explicit–explicit and implicit–explicit staggered time-integrators for highly non-linear compressible fluid–structure interaction problems. International Journal for Numerical Methods in Engineering 2010;84(1):73–107.

[245] Degroote J, Vierendeels J. Multi-level quasi-newton coupling algorithms for the partitioned simulation of fluid–structure interaction. Computer Methods in Applied Mechanics and Engineering 2012;225:14–27.

[246] Bogaers AE, Kok S, Reddy BD, Franz T. Quasi-newton methods for implicit black-box fsi coupling. Computer Methods in Applied Mechanics and Engineering 2014;279:113–32.

[247] Heil M. An efficient solver for the fully coupled solution of large-displacement fluid–structure interaction problems. Computer Methods in Applied Mechanics and Engineering 2004;193(1-2):1–23.

[248] Dettmer WG, Perić D. On the coupling between fluid flow and mesh motion in the modelling of fluid–structure interaction. Computational Mechanics 2008;43(1):81–90.

[249] SBM Offshore, SBM Offshore S3 Wave Energy Converter – watch the video! https://www.sbmoffshore.com/news/sbm-offshore-s3-wave-energy-converter-watch-the-video/; 2020 [Accessed 28 October 2020].

[250] Payne G. Guidance for the experimental tank testing of wave energy converters. SuperGen Marine 2008;254.

[251] Harris RE, Johanning L, Wolfram J. Mooring systems for wave energy converters: A review of design issues and choices. Marec2004 2004;.

[252] Qiao D, Haider R, Yan J, Ning D, Li B. Review of wave energy converter and design of mooring system. Sustainability 2020;12(19):8251.

[253] Ayob MN, Castellucci V, Abrahamsson J, Waters R. A remotely controlled sea level compensation system for wave energy converters. Energies 2019;12(10):1946.

[254] Ferri F, Ambühl S, Fischer B, Kofoed JP. Balancing power output and structural fatigue of wave energy converters by means of control strategies. Energies 2014;7(4):2246–73.

[255] Ambühl S, Kramer M, Sørensen JD. Reliability-based structural optimization of wave energy converters. Energies 2014;7(12):8178–200.

[256] Ambühl S, Ferri F, Kofoed JP, Sørensen JD. Fatigue reliability and calibration of fatigue design factors of wave energy converters. International Journal of Marine Energy 2015;10:17–38.

[257] Zurkinden AS, Lambertsen SH, Damkilde L, Gao Z, Moan T. Fatigue analysis of a wave energy converter taking into account different control strategies. In: International Conference on Offshore Mechanics and Arctic Engineering; vol. 55423. American Society of Mechanical Engineers; 2013, p. V008T09A057.

[258] Kolios A, Di Maio LF, Wang L, Cui L, Sheng Q. Reliability assessment of point-absorber wave energy converters. Ocean Engineering 2018;163:40–50.